

Measurement of A_x and A_z asymmetries in the quasi-elastic ${}^3\text{He}(\vec{e}, e'd)$ reaction

W. Bertozzi, O. Gayou, [S. Gilad](#) (co-spokesperson), P. Monaghan, A. Puckett,
Y. Qiang, A. Shinozaki, Y. Xiao, X. Zhan, C. Zhang
Massachusetts Institute of Technology, Cambridge, Massachusetts

J.-P. Chen, A. Deur, R. Feuerbach, [D. W. Higinbotham](#) (co-spokesperson),
J.-O. Hansen, B. Reitz, A. Saha, B. Wojtsekhowski
Thomas Jefferson National Accelerator Facility, Newport News, Virginia

K. Allada, D. Dale, C. Dutta, A. Kolarkar, [W. Korsch](#) (co-spokesperson)
University of Kentucky, Lexington, Kentucky

M. Potokar, [S. Širca](#) (co-spokesperson) ¹
J. Stefan Institute and Dept. of Physics, University of Ljubljana, Slovenia

G. Cates, R. Lindgren, N. Liyanage, V. Nelyubin, [B. E. Norum](#) (co-spokesperson), K. Wang
University of Virginia, Charlottesville, Virginia

Z.-L. Zhou
Schlumberger-Doll Research, Ridgefield, Connecticut

J. Golak, R. Skibiński, H. Witała
M. Smoluchowski Institute of Physics, Jagiellonian University, Cracow, Poland

W. Glöckle
Institut für Theoretische Physik II, Ruhr Universität Bochum, Bochum, Germany

A. Nogga
Forschungszentrum Jülich, IKP (Theorie), Jülich, Germany

P. Sauer, L. Yuan
University of Hannover, Hannover, Germany

A. Deltuva
University of Lisbon, Lisbon, Portugal

Z.-E. Meziani, B. Sawatzky, P. Solvignon
Temple University, Philadelphia, Pennsylvania

¹Contact person, e-mail: sirca@jlab.org

E. Piasetzky, R. Shneor
Tel Aviv University, Tel Aviv, Israel

J. Glister, A. J. Sarty
Saint Mary's University, Halifax, Nova Scotia, Canada

J. R. M. Annand, D. Ireland, G. Rosner
University of Glasgow, Glasgow, Scotland

S. Choi
Seoul National University, Seoul, South Korea

R. Subedi, J. Watson
Kent State University, Kent, Ohio

L. Weinstein
Old Dominion University, Norfolk, Virginia

and

The Hall A Collaboration

Abstract

This update, along with a copy of the original proposal (attached as Appendix B), is a jeopardy resubmission of experiment E02-108 approved by PAC22.

This is the only Jefferson Lab polarized ^3He experiment which is seeking to better understand the ^3He system, as opposed to using it as an effective neutron target, by measuring double-polarized asymmetries in the $^3\text{He}(\vec{e}, e'd)$ reaction which are believed to be a probe particularly sensitive to the details of the ^3He system. Since the original proposal, major theoretical advances have been made in the Faddeev calculations of the Bochum/Krakow and Hannover groups, resulting in quite distinct descriptions of these observables. This development has important implications for all "neutron" experiments and has rendered the physics case of the experiment even more pertinent.

The recent first successful operation of the BigBite spectrometer at an angle, beam energy, and luminosity very similar to the present proposal has demonstrated that the instrumental requirements of our experiment can be met. We continue to ask for 15 PAC days.

1 Update of the physics case

A variety of ^3He -based experiments seeking to extract neutron information (such as G_E^n and G_M^n , or A_1^n at high x) rely on a virtually perfect theoretical knowledge of the ground-state spin structure of ^3He . The manifestations of S' - and D -state components, specifically the degrees of neutron and proton polarizations within the polarized ^3He nucleus, represent a most important part of this knowledge. Yet, we maintain that the structure of polarized ^3He has not been studied comprehensively enough to accept the extractions performed in these experiments with unreserved confidence.

A direct measurement devoted to a better understanding of the ^3He system *itself* is needed, contrary to the multitude of experiments seeking to extract neutron information *based on* this (incomplete) input. Without a significant improvement in this understanding, future experiments on ^3He and those being analyzed will be seriously impaired. A measurement of a set of double-polarization observables with enough kinematical lever arm is needed in order to constrain the theories. Quantifying the role of the S' and D states in ^3He is one of the key facets of these theories, and thus of the “standard model” of few-body systems. The proponents of the state-of-the-art Faddeev calculations have repeatedly asked for such tests to be done, and the list of References published in the past few years testifies to the intense work invested in the field.

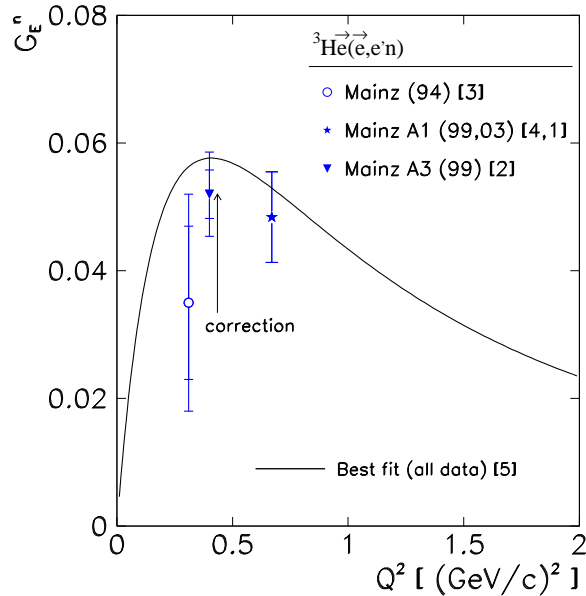


Figure 1: Existing measurements of the neutron charge form-factor using polarized ^3He targets. The size of the theoretical correction needed to interpret the datum at $Q^2 = 0.40 (\text{GeV}/c)^2$ [2] as “neutron” data is shown by an arrow. The datum at $Q^2 = 0.31 (\text{GeV}/c)^2$ [3] has never been theoretically corrected, while the correction for the measurement at $Q^2 = 0.67 (\text{GeV}/c)^2$ [4] was computed to be smaller than 4% [1]. The curves show the Galster refit by Schiavilla and Sick [5] to all existing G_E^n data (primarily double-polarized measurements on the deuteron).

To re-illustrate these points, Figure 1 first shows the presently available data on the neutron charge form-factor as extracted from the quasi-elastic ${}^3\text{He}(\vec{e}, e'n)$ reaction. The data set presented in this figure has changed only insignificantly since our original proposal [1]. At low values of Q^2 where final-state interactions in this process are most relevant, the differences between the plane-wave, symmetrized plane-wave, and the full Faddeev calculation with complete wave-functions is significant. Furthermore, while the effects of small wave-function components at the cross-section level are believed to be small, this is certainly not the case in the double-polarized asymmetries through which the form-factors are extracted.

As an additional example, Fig. 2 shows the error budget of the recently completed E99-117 experiment in which A_1^n was extracted. Aside from the statistical uncertainty, the leading error source is the uncertainty of the polarization of the proton and neutron ($P_p P_n$ label in the Figure) in polarized ${}^3\text{He}$. These polarizations relate intimately to the corresponding components of the ${}^3\text{He}$ wave-function. In E99-117, the statistical uncertainty dominates, but it will become comparable to or even smaller than the uncertainty in P_p and P_n for the A_1^n measurement with CEBAF at 11 GeV (shaded band). Note that a correction in P_p or P_n would imply a shift of *all* points up or down, thus changing completely the interpretation of the zero crossing of $A_1^n(x)$.

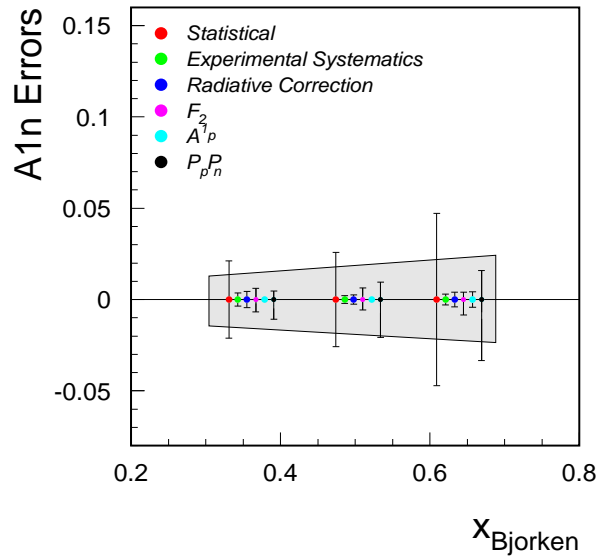


Figure 2: Summary of uncertainties in E99-117, with $P_p P_n$ denoting the error due to uncertainties in the effective proton and neutron polarizations in polarized ${}^3\text{He}$. The shaded band shows the expected statistical error of the 11 GeV measurement, which is comparable to or even smaller than the error in $P_p P_n$.

The precision of various double-polarization experiments has thus obviously reached a level that needs to be matched by the best theoretical models of the ${}^3\text{He}$ nucleus. These models in turn require increasingly accurate input to adjust their parameters like the ground-state wave-function components, and a complete understanding of the spin and isospin dependence of the reaction-mechanism effects such as final-state interactions (FSI) and meson-exchange currents (MEC). Preferably, all these ingredients should be studied in a broad kinematic range to increase the lever arm.

However, although the theoretical corrections described above appear to be under control and are commonly assumed to be well understood, we show below that large discrepancies persist among the two best “standard” models on related specific double-polarization observables. In fact, the disagreements between the theoretical predictions on the recoil-momentum dependencies of transverse asymmetries A_x and A_z for double-polarized two-body electro-disintegration of ${}^3\text{He}$ has increased since the preparation of our original proposal, in spite of the fact that both theory groups (Bochum/Krakow and Hannover) have reportedly improved their individual approaches. Such discrepancies, prominent even at small recoil momenta, cast a shadow of uncertainty over the extractions of both electric and magnetic neutron form-factors.

We believe that theoretical disagreements of such magnitude must be rectified and are convinced that our experiment, virtually in its original form and scope, will directly improve our understanding of the ${}^3\text{He}$ system. The parasitic measurement of G_E^n described in Appendix A adds further value as a means of normalization at small missing momentum, and enhances the experiment’s overall capacity to constrain theories. As a whole, the experiment remains an excellent calibration method for models upon which many data interpretations rest. Without a significant improvement in this understanding, future experiments on ${}^3\text{He}$ shall remain incomplete.

2 Advances in theory

2.1 Bochum/Krakov Group

Since the submission of the original proposal, major theoretical advances have been made in the non-relativistic Faddeev calculations of the Bochum/Krakov Group [8–10], in particular in the treatment of the MEC and the three-nucleon force (3NF). The non-relativistic approach is justified since the three-nucleon center-of-mass energy remains below the pion threshold and the total three-nucleon lab momentum is smaller than the nucleon mass. In such kinematics the NN forces are well tuned, while the parameters of the 3NF are adjusted to the trinucleon binding energies. However, the authors warn that an appropriate and conclusive test of the interplay of the NN and 3N forces as well as FSI for electron-induced inelastic processes on ${}^3\text{He}$ has not yet been established.

The Bochum/Krakov group maintains that the double-polarized electron-induced two-body breakup of ${}^3\text{He}$ provides an exceptionally rich playground to test the nuclear dynamics, and that a successful description of all observables requires a full list of dynamical ingredients in a consistent calculation. The two-body breakup ${}^3\text{He}(\vec{e}, e'd)$ is particularly interesting because of the interference of the PWIA proton process and the deuteron process, together constituting PWIAS with the symmetrized final state and resulting in quite distinct proton vs. deuteron angular or recoil-momentum distributions, respectively (see [9] for details). It is important to investigate the interplay between the two channels with full inclusion of rescatterings by studying the angular (or recoil-momentum) dependence of the cross-section and of double-polarization observables.

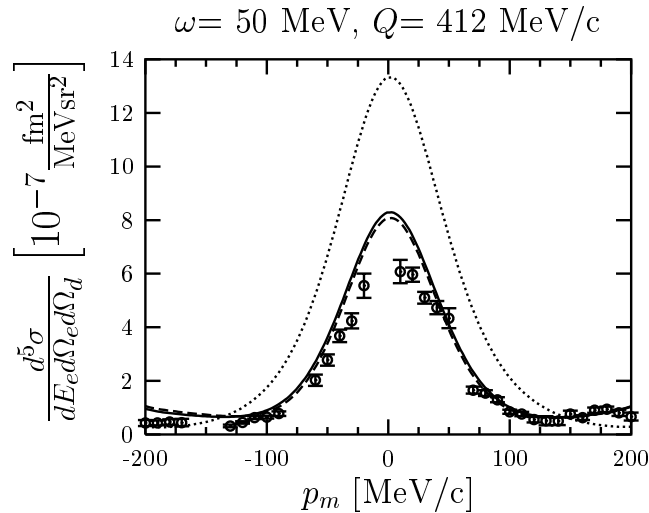


Figure 3: Measured recoil-momentum dependence of the cross-section for the unpolarized ${}^3\text{He}(e, e'd)$ process [11] compared to the Bochum/Krakov calculation: PWIAS (dotted), full without MEC (dashed) and full (full curves).

For proton knockout, the theory is expected to perform well at both low and high Q . At low Q , the FSI play a role, but the nuclear forces used in the calculations describe pd -scattering well, and MEC effects are very small. On the other hand, at high Q , PWIA represents just an overlap of the deuteron and the ${}^3\text{He}$ state at relatively low deuteron momenta. Yet, a precise set of data over the entire angular region is still lacking. The situation is even more interesting in the case of deuteron knockout, where recently published cross-section data [11] exhibits a strong discrepancy with respect to the theory (see Fig. 3). At present, it is not clear which ingredient of the calculation may be responsible for the disagreement which is generated mostly through the longitudinal part of the cross-section. Use of the Sachs form-factors G_E^p and G_E^n instead of the Pauli form-factors F_1^p and F_1^n , the three-nucleon force, as well as the inclusion of MEC in the charge-density operator are some candidates (see [11] for details). Our measurement will in addition provide unpolarized cross-sections with accuracy surpassing the NIKHEF data as an additional cross-check.

In the following, we describe the most recent calculations of the Bochum/Krakow Group performed specifically for our experiment. For the definitions of the asymmetries A_x and A_z see page 10 of Appendix B.

The calculations for the original proposal were done with an incomplete treatment of MEC, and without 3NF effects. Now these dynamical components have been included more rigorously. The Group uses the AV18 nucleon-nucleon force, and the UrbanaIX three-nucleon force. Figure 4 shows the dependence of the results for A_x and A_z on the dynamical ingredients used in the calculation. In the 3NF calculations, the three-nucleon force is employed in both bound and scattering states.

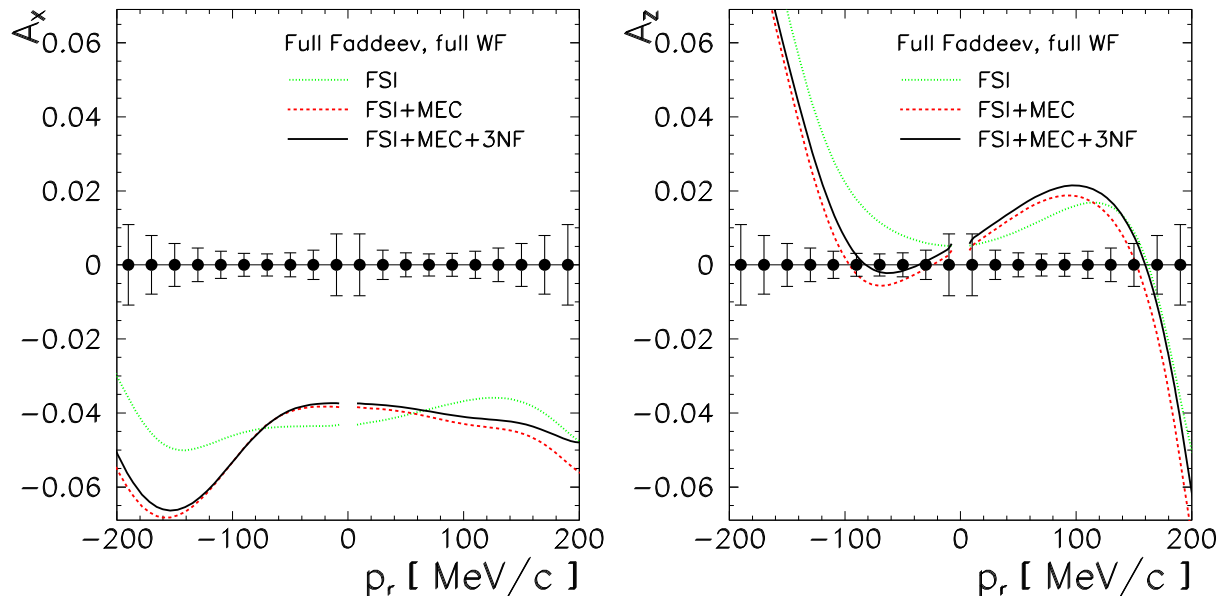


Figure 4: Bochum/Krakow full Faddeev calculations in perpendicular kinematics, with full wave-function, showing the dependence on included ingredients (FSI, MEC, 3NF). The 3NF effect is not negligible, but it is relatively small. Our expected statistical uncertainties are also shown.

Manifestations of small ${}^3\text{He}$ wave-function components represent a major focus of our experiment. The Bochum/Krakow Group has therefore provided us with the asymmetry calculations with truncated ${}^3\text{He}$ wave-functions (i.e. without S' and D states). A possible general problem entailed in this procedure is that the wave-function components are generated via given nuclear forces, and thus a deliberate omission of a part of the wave-function can introduce inconsistencies in the treatment of the three-nucleon scattering state. Nevertheless, Figure 5 shows the dependence of A_x and A_z on the ${}^3\text{He}$ wave-function truncation. Only the dominant components (S , S' , and D) have been used. The P component which enters the ground-state probabilities at a 0.1 % level (see [12]) gives a negligible contribution and has been omitted.

In Fig. 5, we therefore identify

S only	${}^3\text{He}$ wave-function restricted to principal S -state,
$S+S'$	${}^3\text{He}$ wave-function without the D -state,
$S+D$	${}^3\text{He}$ wave-function without the S' -state,
Full WF	Full ${}^3\text{He}$ wave-function.

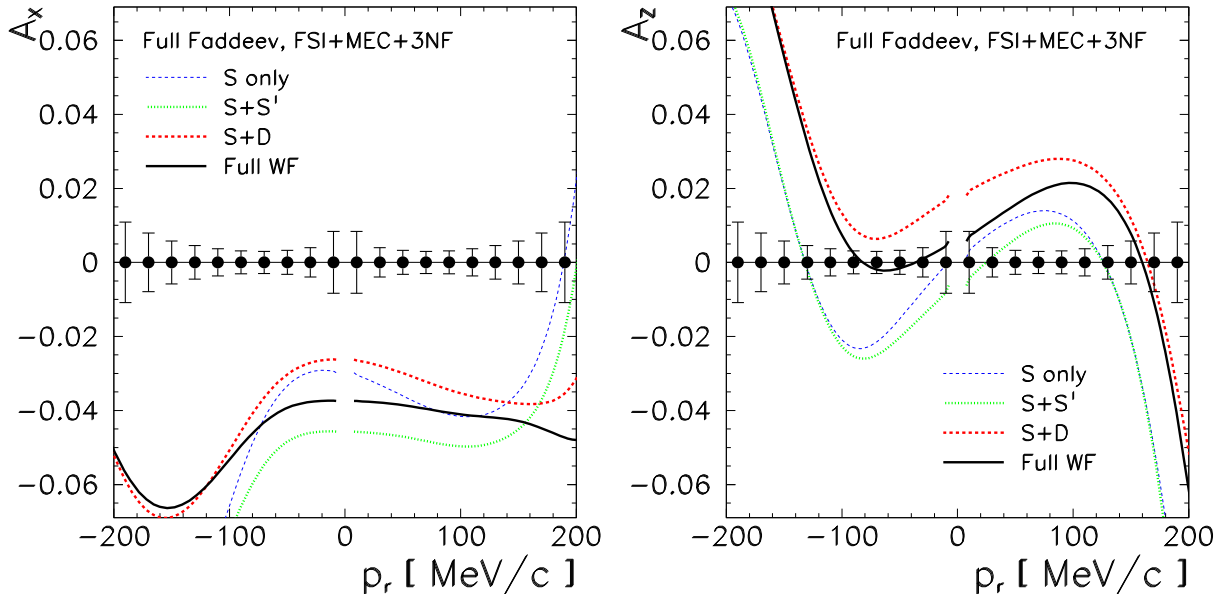


Figure 5: Bochum/Krakow full Faddeev calculations, with FSI, MEC, and 3NF, showing the effect of wave-function component truncation, ignoring the negligible contribution of the P state. Our expected statistical uncertainties are also shown.

The trends shown in Fig. 5 re-establish the trends described in the original proposal. In A_x , at small p_r , one does observe a larger change in the asymmetry when one goes from (S only) to ($S + S'$). On the other hand, it is evident that it is the D -state that brings A_x down into the vicinity of the (Full) curve. The same conclusion applies to A_z .

The sensitivity to the “amount” of S' can be estimated crudely by interpolating between the (Full) and ($S + D$) curves, and extrapolating into the surrounding region. Assuming that the full wave-function contains 1.24% S' (see Refs. [12,13]), Fig. 6 shows the result of this procedure.

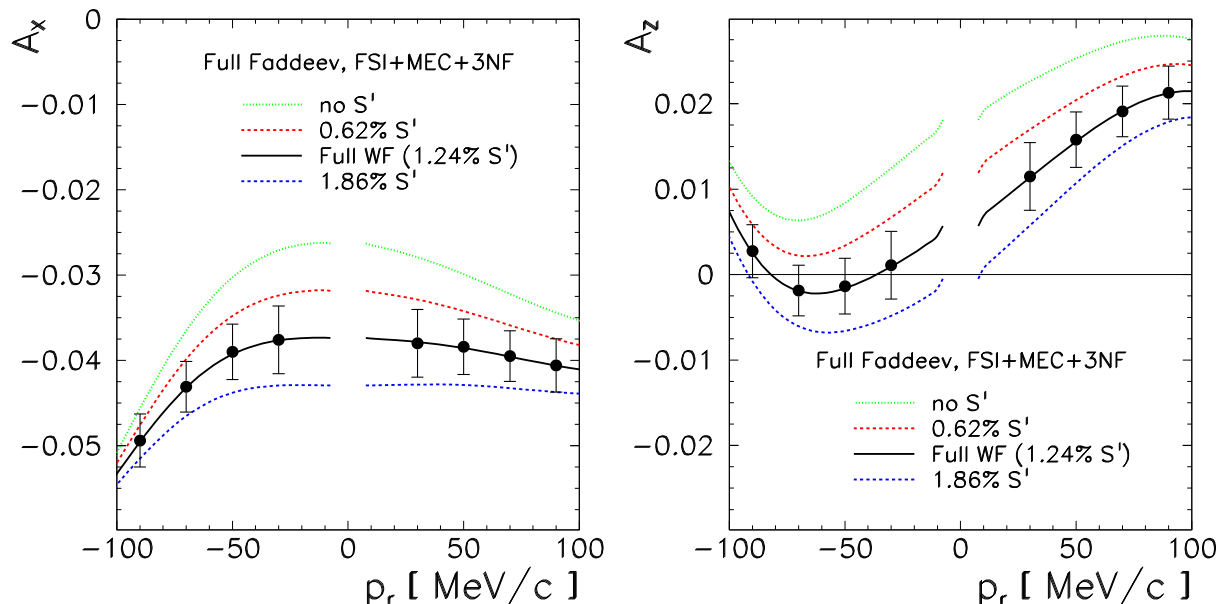


Figure 6: A naive estimate of the sensitivity of A_x and A_z on the “amount” of the S' component in the ${}^3\text{He}$ wave-function. The estimate of 1.24% of the S' state in the full wave-function is as reported by [12,13]. Our expected statistical uncertainties are also shown.

Of course, it is the interferences of the wave-function components that govern the p_r -behavior of the asymmetries, and in practice, the “amount” of S' can not be determined without model dependence in the simple way described here. However, note that in spite of it being so simple, this method is not unlike the one invoked in the extraction of G_E^n from measured asymmetry data. In addition, our experiment will cover an exceptionally large kinematic range, such that a realistic theory will be strained to match the broad span of data throughout which small wave-function components enter at different places. The Bochum/Krakow group themselves have repeatedly asked for just such a benchmark comparison on double-polarized two-body electro-disintegration of ${}^3\text{He}$.

2.2 Hannover Group

Faddeev calculations of the two-body and three-body breakups of ${}^3\text{He}$ by the Hannover Group also include FSI and MEC, and the theoretical apparatus is presumed to be comparable to the one used in Bochum/Krakow. However, the Hannover Group adds the Δ isobar as an active degree of freedom providing a mechanism for an effective three-nucleon force and for exchange currents. Since the inception of our original proposal, the Group has also gradually incorporated several refinements into their calculations [14–18].

For the calculations used in the original proposal [14, 15], a separable expansion of the Paris potential was used. In the latest calculations [16–18], the three-particle scattering equations are solved exactly by using a Chebyshev expansion of the two-baryon transition matrix as the interpolation method. The underlying purely nucleonic reference potential is the charge-dependent CD Bonn potential. A coupled-channel extension of the CD Bonn potential has been developed and refitted; it was shown to be just as realistic as the original CD Bonn. Furthermore, the point Coulomb interaction is added in the partial waves involving two charged baryons. The Figures below follow the notation

CD Bonn	CD Bonn potential exactly as in [18],
CD Bonn + Coulomb	added Coulomb (see text),
CD Bonn + Coulomb + Δ	added Δ , coupled channels (see text).

Figure 7 shows the current results of the Hannover calculation for our experiment. Two calculations involving one-nucleon currents only (CD Bonn and AV18, neglecting charge dependence) are also shown.

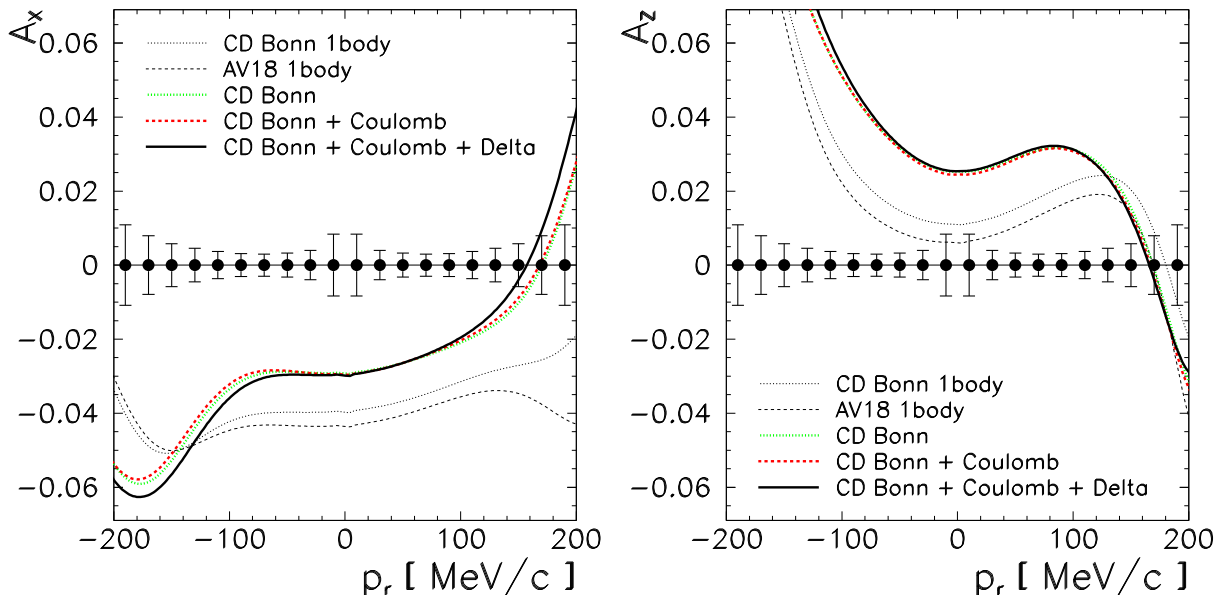


Figure 7: Hannover Group calculations showing different ingredients of the calculations (for details, see text). Our expected statistical uncertainties are also shown.

2.3 Comparison Bochum/Krakov vs. Hannover

Although the calculations of the Bochum/Krakov and Hannover Group have been cross-checked in many instances [19], there are marked differences between them in the case of transverse asymmetries for ${}^3\text{He}(\vec{e}, e'd)$. Figure 8 shows the comparison between the state-of-the-art predictions of both Groups. Our experiment will help significantly in diminishing the differences between these two theoretical approaches.

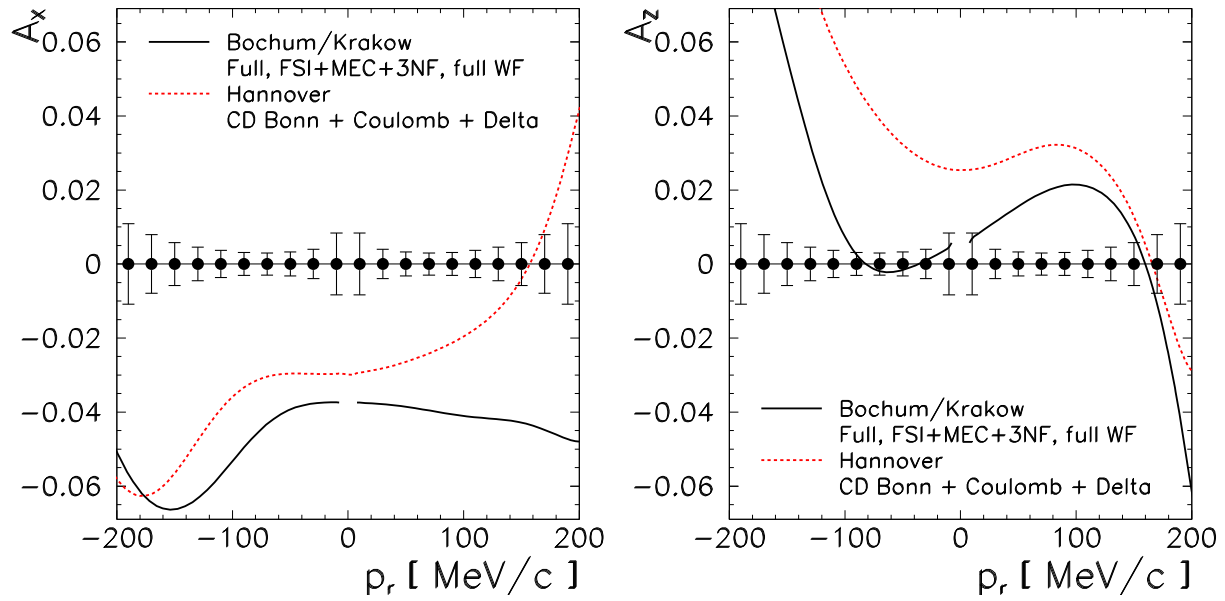


Figure 8: State-of-the-art Bochum/Krakow vs. state-of-the-art Hannover. With the more detailed inclusion of MEC and 3NF, the Bochum/Krakow A_x has flattened out at positive p_r , while A_z has come closer to zero at negative p_r . The Hannover curves have not changed significantly upon inclusion of Coulomb effects and adopting a different NN potential.

3 Advances in experiment

3.1 BigBite instrumentation

Since this experiment was first approved, the BigBite spectrometer has evolved from a work-in-progress to a fully operational system (see Fig. 9). The first experiment to use the BigBite spectrometer, the Short-Range Correlations (SRC) experiment E01-015, was installed in December of 2004 and ran through March of 2005. The next BigBite experiment, which will measure the electric form-factor of the neutron at high Q^2 , is being prepared now and will run in early 2006. For the ${}^3\text{He}(\vec{e}, e'd)$ experiment, we will use the Hall A left high-resolution spectrometer for detecting the scattered electrons and the large-acceptance BigBite spectrometer for detecting the scattered deuterons.

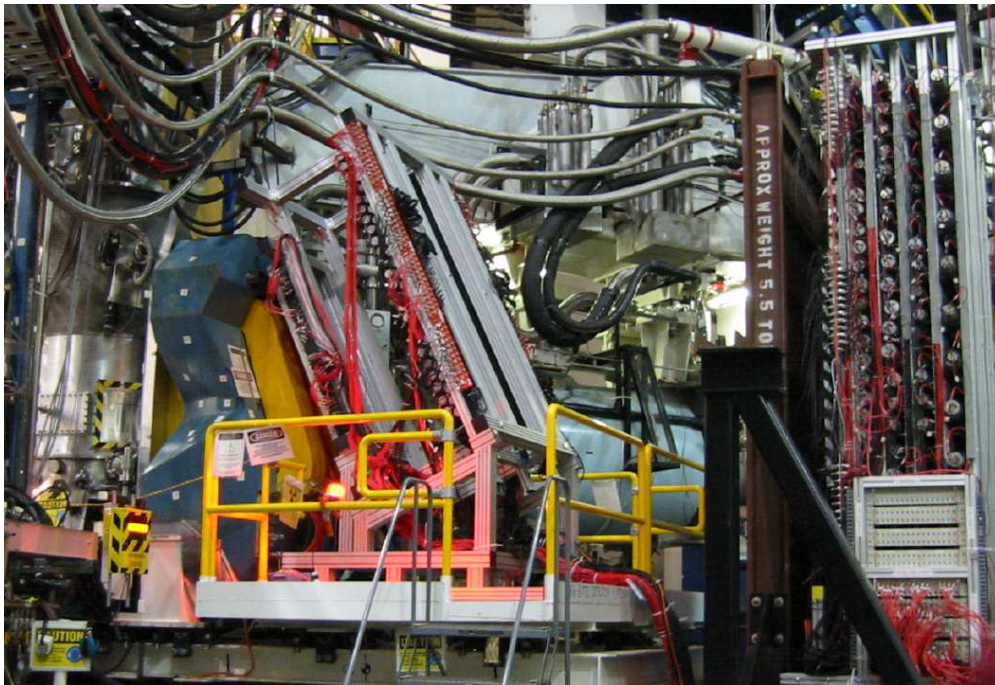


Figure 9: A picture of the BigBite spectrometer installed in Hall A during the E01-015 SRC experiment. The blue BigBite dipole can be seen on the left, followed by the SRC hadron detector package. On the right is the neutron detector used during E01-015 and will be available for a parasitic measurement of the quasi-elastic $(e, e'n)$ reaction (see Appendix A).

3.2 Particle identification

One critical issue related to the ${}^3\text{He}(\vec{e}, e'd)$ experiment is a clean discrimination of deuterons from protons. During the E01-015, the BigBite spectrometer was positioned at 70° and was run at a beam energy of 2.2 GeV, a kinematics very similar to this proposal (70° ,

2.4 GeV, respectively). Fig. 10 shows a timing spectrum from this kinematics and demonstrates that even with an uncorrected time-of-flight spectrum, the separation between protons and deuterons is rather clean. To further sharpen up the spectrum, a momentum correction will be applied to the raw timing. In addition, the dE/E information from both the thin and thick layers of the trigger scintillator planes can be used for particle identification.

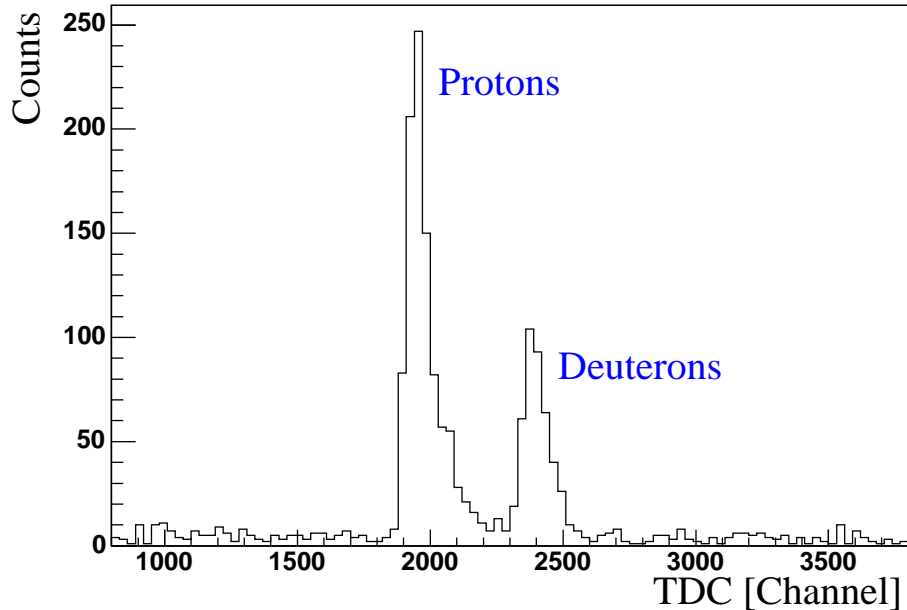


Figure 10: Particle identification in BigBite via time-of-flight (uncorrected on-line spectrum). The discrimination will improve with momentum corrections and by using dE/E information.

3.3 Rate estimates

Detailed count-rate estimates can be found in the original proposal. From the rate tests done during the SRC experiment and the tests that have been done for the upcoming G_E^n measurement at high- Q^2 , it appears that excessive rates are no longer an issue for this particular experiment. We will run at the same low luminosity as the upcoming G_E^n experiment, but in our experiment BigBite will be at a larger angle (70° as opposed to 50°), and at a lower beam energy. Moreover, we will be using a high-resolution spectrometer to detect the electron and to form the trigger, whereas the G_E^n experiment must use BigBite and the neutron array to this purpose. Additionally, we will be using BigBite to detect low-energy hadrons, which will allow us to set relatively high discriminator thresholds in the BigBite trigger plane.

4 Conclusion

Since the submission of the original proposal, tremendous progress has been made in the theoretical description of the ${}^3\text{He}$ system, and this knowledge has been widely used in interpretations of ${}^3\text{He}$ experiments to provide access to neutron information. However, disagreements between these state-of-the-art theories in double-polarized observables, and even some discrepancies between unpolarized data and theories, persist and indicate that a sufficient understanding of this fundamental nuclear system has not yet been achieved.

We are re-proposing an experiment which is directly aimed at a better understanding of the ${}^3\text{He}$ system, as opposed to using it as an effective neutron target. Still, these two viewpoints are not disjunct as the two systems need to be understood simultaneously in the framework of a single theory, preferably in a broad kinematic range. Our measurement of the recoil-momentum dependence of double-polarization asymmetries in the ${}^3\text{He}(\vec{e}, e'd)$ reaction is an experiment designed with exactly these requirements in mind. The simultaneous precision measurement of G_E^n (see Appendix A) will provide an additional valuable cross-check. These measurements will provide a set of constraints on theories severe enough to significantly further our knowledge of the ground-state structure of ${}^3\text{He}$, as well as to increase the reliability of extracting neutron information based on it.

We continue to ask for 15 PAC days.

References

- [1] J. Bermuth et al., Phys. Lett. B **564** (2003) 199.
- [2] J. Becker et al., Eur. Phys. J. A **6** (1999) 329.
- [3] M. Meyerhoff et al., Phys. Lett. B **327** (1994) 201.
- [4] D. Rohe et al., Phys. Rev. Lett. **83** (1999) 4257.
- [5] R. Schiavilla, I. Sick, Phys. Rev. C **64** (2001) 041002.
- [6] C. Carasco et al. (A1 Collaboration), Phys. Lett. B **559** (2003) 41.
- [7] P. Achenbach et al. (A1 Collaboration), nucl-ex/0505012.
- [8] J. Golak et al., Phys. Rev. C **65** (2002) 064004.
- [9] W. Glöckle et al., Eur. Phys. J. A **21** (2004) 335.
- [10] J. Golak et al., nucl-th/0505072.
- [11] C. M. Spaltro et al., Nucl. Phys. A **706** (2002) 403.
- [12] R. Schiavilla et al., Phys. Rev. C **58** (1998) 1263.
- [13] A. Kievsky, M. Viviani, S. Rosati, Phys. Rev. C **52** (1995) R15.
- [14] L. P. Yuan et al., Phys. Rev. C **66** (2002) 054004.
- [15] L. P. Yuan et al., Few-Body Systems **32** (2002) 83.
- [16] A. Deltuva, R. Machleidt, P. U. Sauer, Phys. Rev. C **68** (2003) 024005.
- [17] A. Deltuva et al., Phys. Rev. C **69** (2004) 034004.
- [18] A. Deltuva et al., Phys. Rev. C **70** (2004) 034004.
- [19] J. Golak, P. Sauer, A. Deltuva, Private Communications.
- [20] J. Friedrich and Th. Walcher, Eur. Phys. J. A, **17** (2003) 607.
- [21] J. Golak et al., Phys. Rev. C **63** (2001) 034006.
- [22] R. W. Schulze and P. U. Sauer, Phys. Rev. C **48** (1993) 38.

A Parasitic measurement of G_E^n

The experiment proposed here is optimized for ${}^3\vec{\text{He}}(\vec{e}, e'd)$ in quasi-elastic (QE) kinematics with an incident beam energy of 2.4 GeV. Due to the large angular acceptance of BigBite and a $\pm 4\%$ momentum acceptance of the HRS, it is feasible to detect a sizeable fraction of the quasi-elastic ${}^3\vec{\text{He}}(\vec{e}, e'n)$ pp process with the HRS and the neutron detector of BigBite. This kinematic region can be used to tap the main experiment parasitically in order to extract G_E^n at $Q^2 = 0.36 \text{ (GeV/c)}^2$ with high precision and *for free*. The chosen value of Q^2 is in the vicinity of the maximum (see Fig. 1) where additional precise data is mostly needed to pin down the functional shape of G_E^n . This additional determination will not only aid the G_E^n effort; it is also quite instrumental in achieving the goals of the present proposal in the manner described in the main text.

The central angle of BigBite will be 72.8° while the optimal angle for G_E^n extraction is 64.2° . The angular acceptance of the BigBite neutron detector is roughly from 68° to 78° . The central momentum of the HRS will be $E' = 2.294 \text{ GeV}$, while the correct E' for the QE process is 2.201 GeV , near the edge of the HRS momentum acceptance. These mismatches notwithstanding, we are still able to cover the low-energy side of the QE peak which can be used for a high-precision extraction of G_E^n .

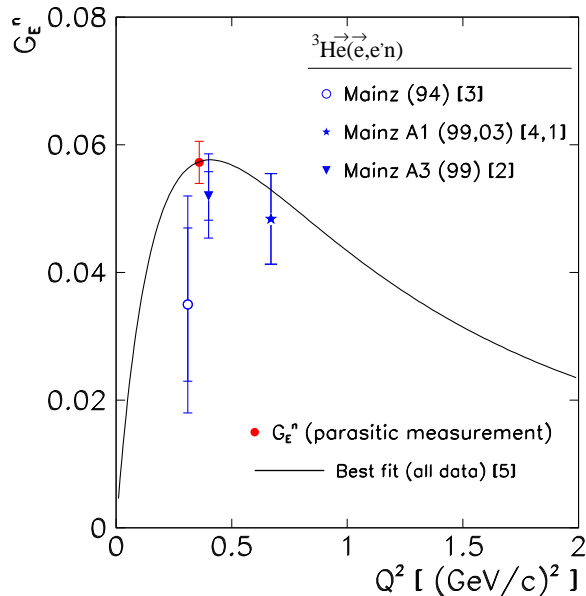


Figure 11: The expected statistical uncertainty of the parasitic measurement of G_E^n at $Q^2 = 0.36 \text{ (GeV/c)}^2$.

The count-rate estimates for the parasitic measurement were performed by using a Monte Carlo simulation with the ${}^3\text{He}$ spectral function by Schulze and Sauer [22], and by assuming a 20 cm useful target length. The expected neutron rate is 20 Hz assuming a neutron detection efficiency of 0.2. Since the main experiment plans to spend $\approx 2 \times 7$ days in parallel and perpendicular kinematics, a total of $\approx 12 \times 10^7$ neutrons will be detected for each target spin configuration. The statistical uncertainties in the measured asymmetries are: $dA_\perp/A_\perp = 2.1\%$ and $dA_\parallel/A_\parallel = 0.42\%$. This means that the total uncertainty

in the extraction of G_E^n is entirely dominated by systematic and theoretical uncertainties. Assuming a 2.5% uncertainty for the beam polarization, 3.5% for the target polarization, and 0.03 in the knowledge of G_M^n (which is the dominant uncertainty), G_E^n can be determined to an accuracy of better than 0.0039. If both perpendicular and longitudinal asymmetries are taken into account, the uncertainty can be improved to about 0.0033 (the ratio method). The expected precision is shown in Fig. 11.

The main source of background is the $(e, e'p)$ reaction. The expected total proton rate on the neutron detector would be ≈ 730 Hz (30 Hz from two-body and 700 Hz from three-body break-up), if no magnetic field (BigBite dipole), PID- or veto-detectors were present. We expect to be able to reduce the proton background to a negligible level (see subsection 3.2 particle ID).

B Copy of original proposal E02-108

Hall A Proposal to JLab PAC 22

May 27, 2002

Measurement of A_x and A_z asymmetries in the quasi-elastic ${}^3\text{He}(\vec{e}, e'd)$ reaction

W. Bertozzi (co-spokesperson), Z. Chai, O. Gayou, S. Gilad, P. Monaghan,
M. Rvachev, R. Suleiman, Y. Xiao, B. Zhang, X. Zheng, Z.-L. Zhou (co-spokesperson) ¹
Massachusetts Institute of Technology, Cambridge, Massachusetts

J.-P. Chen, D. W. Higinbotham (co-spokesperson), J.O. Hansen, B. Reitz,
A Saha, B. Wojtsekhowski
Thomas Jefferson National Accelerator Facility, Newport News, Virginia

S. Širca (co-spokesperson)
University of Ljubljana, Ljubljana, Slovenia

G. Cates, A. Deur, R. Lindgren, B. E. Norum (co-spokesperson), B. Sawatzky, K. Wang
University of Virginia, Charlottesville, Virginia

L. Weinstein
Old Dominion University, Norfolk, Virginia

A.J. Sarty
Saint Mary's University, Halifax, Nova Scotia, Canada

V. Nelyubin
St. Petersburg Nuclear Physics Institute, Gatchina, Russia

F. Butaru, S. Choi, Z.-E. Meziani, N. Ploquin, P. Solvignon, H. Yao
Temple University, Philadelphia, Pennsylvania

J. R. M. Annand, D. Hamilton, D. Ireland
University of Glasgow, Glasgow, Scotland

P. Sauer, L. Yuan
University of Hannover, Hannover, Germany

W. Korsch, P. Zolnierczuk
University of Kentucky, Lexington, Kentucky

and

The Hall A Collaboration

¹Contact person, e-mail: zzhou@lns.mit.edu

Abstract

We propose a study of the quasi-elastic ${}^3\text{He}(\vec{e}, e'd)p$ reaction in Hall A with the polarized ${}^3\text{He}$ target in conjunction with the High-Resolution Spectrometers and the large-acceptance BigBite spectrometer. The purpose of this measurement is to test the state-of-the-art Faddeev calculations of the three-body system and to study the S' -state and D-state contributions to the ${}^3\text{He}$ ground-state wave-function.

Beam-target asymmetries A_x and A_z will be measured in the range of recoil momenta p_r from 0 to about 200 MeV/c, in both parallel and perpendicular kinematics. At $p_r \lesssim 70$ MeV/c, the D state will be highly suppressed and the asymmetries will be uniquely sensitive to the interference of the S and S' states. At larger recoil momenta, the contribution of the D state will be increasingly important. We request 15 days of 2.4 GeV, 12 μA polarized electrons in order to perform this experiment.

This proposal is based on the favorable deferral by PAC 21 (see Appendix A) and the PAC 20 letter of intent report (see Appendix B). This proposal has been endorsed by the Hall A collaboration and has received strong theoretical support from the Bochum and Hannover groups. The requested beam-time has been reduced by limiting the experiment to one position of the BigBite spectrometer. While this means a slightly smaller range in perpendicular missing momenta will be covered, it removes the overhead of moving and surveying the spectrometer during the experiment and helps reduce calibration issues, since only one location and central momentum of the BigBite spectrometer will be needed.

Contents

1	Introduction	4
2	Physics motivation	5
2.1	Overview of existing related measurements	7
2.2	Relation to Jefferson Lab experiments	8
2.3	Relation to Bates and Mainz experiments	8
3	Formalism of the ${}^3\text{He}(\vec{e}, e'd)p$ reaction	10
3.1	Choice of kinematics	10
4	Experimental equipment and methods	16
4.1	Polarized ${}^3\text{He}$ target	17
4.2	$\vec{e}-{}^3\text{He}$ elastic scattering as a polarization monitor	18
4.3	High-Resolution Spectrometers	19
4.4	BigBite Spectrometer	19
5	Count rates and beam time request	21
6	Summary	25
A	PAC 21 proposal report	26
B	PAC 20 letter of intent report	27
	References	28

1 Introduction

The ^3He nucleus is the subject of considerable current interest. It is a calculable nuclear system where our theoretical understanding of its nuclear structure can be compared with data to an increasingly accurate degree [1]. In addition, it is generally thought that polarized ^3He can serve as an effective polarized neutron target for experiments in nuclear and particle physics [2–4]. So far, the experiments have succeeded in imposing only loose constraints on the fundamental properties of the neutron such as its charge, magnetism, and spin distributions. Thus, many experiments using polarized ^3He targets have been performed or are underway, mostly devoted to measurements of neutron elastic form factors [5–8] and deeply-inelastic structure functions [9–11].

Non-relativistic Faddeev calculations [3, 12, 13] of the three-body bound state predict that three components dominate the ^3He ground-state wave-function. The dominant component of the ^3He wave function is the spatially symmetric S state, in which the proton spins are in the spin-singlet state (anti-parallel) and the ^3He spin is predominantly carried by the neutron. This configuration accounts for $\simeq 90\%$ of the spin-averaged wave-function, and its dominance is supported by the near equality of the ^3He and neutron magnetic moments ($\mu_{^3\text{He}} = -2.12$ n.m. and $\mu_n = -1.91$ n.m.). An additional $\simeq 8\%$ of the spin-averaged wave-function can be attributed to the D state generated by the tensor component of the nucleon-nucleon force. In this case, the three nucleon spins are predominantly oriented opposite to the ^3He nuclear spin. The remaining $\simeq 2\%$ originate in a mixed-symmetry configuration of the nucleons, the S' state. It arises because of the differences between the $T = 0$ and $T = 1$ forces and hence reflects (spin-isospin)-space correlations [14]. Results of three-body calculations [15] show that the probability for the S' state is correlated with the binding energy as $P_{S'} \approx E_b^{-2.1}$ ($P_{S'}$ in units of percentage and E_b in units of MeV). The S' state obviously does not exist for ^2H , for the three-body isospin doublet one has $P_{S'} \approx 1 - 1.5\%$, whereas for ^4He and heavier nuclei it is expected to be strongly suppressed, with $P_{S'} < 0.1\%$ due to the higher binding energies. All other components of the ^3He ground-state wave-function are predicted to be negligible.

In this physical picture, polarized ^3He represents an effective polarized neutron target. Several experiments based on this idealization have been performed with the goal of studying the spin structure of the neutron (for example, experiments E142 [9], E154 [10] at SLAC and HERMES [11] at DESY). Related experiments are in preparation or underway at Bates [16], Mainz [17], and JLab [18–24].

2 Physics motivation

The physics motivation of the proposed experiment is very simple and twofold:

- Detailed knowledge of the ground-state spin structure of ${}^3\text{He}$ is crucial to extract precise information on neutron structure from the measurements outlined in the introduction. The S' state is an important part of this knowledge.
- Understanding the role of the D and S' states in ${}^3\text{He}$ is one of the key facets of the “standard model” of few-body theory. In particular, the manifestations of the S' state constitute a stringent test of the state-of-the-art Faddeev calculations.

For applications such as the extraction of precise information on the neutron electromagnetic form factors, it is imperative to understand the ground-state spin structure of the ${}^3\text{He}$ nucleus. To illustrate the point, Figure 1 shows the presently available data on the neutron charge form-factor using quasi-elastic ${}^3\text{He}(\vec{e}, e'n)$ scattering. At low values of Q^2 where final-state interactions in this process are most prominent, the differences between the plane-wave calculation and the calculation with full Faddeev wave-functions exceed the presently achievable experimental uncertainties by factors of two to three. The precision of these double-polarization experiments has reached a level that can only be matched by the best theoretical models of the ${}^3\text{He}$ nucleus. These in turn require increasingly accurate input on its ground-state wave-function components and a complete understanding of the spin and isospin dependence of the reaction-mechanism effects such as final-state interactions (FSI) and meson-exchange currents (MEC). Without this knowledge, all future experiments on ${}^3\text{He}$ at low Q^2 will be seriously impaired.

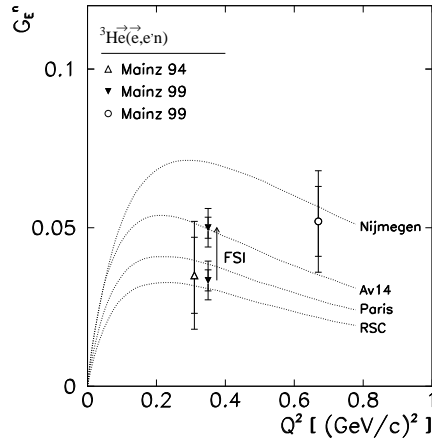


Figure 1: Existing measurements of the neutron charge form-factor using polarized ${}^3\text{He}$ targets. The size of the theoretical correction needed to interpret the datum at $Q^2 = 0.35 (\text{GeV}/c)^2$ [7] as “neutron” data is shown by an arrow. The datum at $Q^2 = 0.31 (\text{GeV}/c)^2$ [6] has never been theoretically corrected, while the correction for the measurement at $Q^2 = 0.67 (\text{GeV}/c)^2$ [8] was estimated to be small. The curves show extracted value of G_n^E from deuteron elastic data for different NN-potentials and are plotted for visual reference.

Clearly there are several corrections to the naive picture of the effective neutron target. For example, the protons in ${}^3\text{He}$ can be partly polarized due to the presence of the S' - and D-state components. The FSI of neutrons with an unpolarized proton pair causes a $\sim 15\%$ reduction of the ${}^3\text{He}(e, e'n)$ cross-section and a corresponding dilution of the G_E^n asymmetry. In contrast, polarized protons will manifest themselves through the FSI and distort (not just dilute) the neutron channel asymmetries. This is one of the reasons that the FSI contributes (even in the region of small p_r) about a 70% correction for the datum at $Q^2 = 0.35 \text{ (GeV/c)}^2$ [7]. The S' state is therefore a small, but important quantity that deserves experimental investigation. It is also well known that the bulk of the difference in charge radii (or diffraction minima of the charge form-factor) of ${}^3\text{H}$ and ${}^3\text{He}$ can be explained by inclusion of the isovector charge current and a correction due to the presence of the S' state [14].

The high level of interest has been illustrated in an extensive experimental [25–27] and theoretical [28–31] effort to study unpolarized ${}^3\text{He}(e, e'd)$ at Bates and NIKHEF. These early experiments have revealed detailed information on nucleon momentum distributions, isospin structure of the currents and on final-state effects. They have also proven the success of the full Faddeev calculations. However, unpolarized measurements lacked the power to isolate small components of the ${}^3\text{He}$ ground-state wave-function (in particular, the S' state) dominating in the region of small recoil momenta, which has the potential to further constrain theoretical models.

Recent investigations of spin asymmetries in quasi-elastic scattering of polarized protons on polarized ${}^3\text{He}$ [32,33] have also provided momentum distributions of proton and neutrons through measurements of two-body and three-body break-up channels ${}^3\vec{\text{He}}(\vec{p}, 2p)$ and ${}^3\vec{\text{He}}(\vec{p}, pn)$. Although innovative and fruitful, this approach revealed its weaknesses inherent to the use of hadronic probes, and helped initiate an investigation of spin-dependent momentum distributions using electron scattering in extended ranges of missing momenta and momentum transfers, and with greater resolving power.

Consequently, the effort to disentangle the effects of small wave-function components has shifted to two-body electro-disintegration of polarized ${}^3\text{He}$ [34–36]. It has been shown [37–41] that the ${}^3\vec{\text{He}}(\vec{e}, e'p)pn$ reaction and especially the ${}^3\vec{\text{He}}(\vec{e}, e'd)p$ channel can provide direct and precise information on both small (S' and D) components of the ${}^3\text{He}$ ground-state wave-function. Large sensitivities have been established both in the diagrammatic approach of Nagorny [38, 41], as well as in two independent full Faddeev calculations of the Bochum group [39] and the Hannover group [40].

Figure 2 shows the leading diagrams for the ${}^3\text{He}(e, e'd)p$ reaction [38]. Diagram a) with the proton pole corresponds to the plane-wave impulse approximation. Diagram b) with the deuteron pole corresponds to the quasi-deuteron model. Together with the ${}^3\text{He}$ -pole and contact diagrams they form the minimal set needed for isoscalar current conservation. For these diagrams the isospin state of the pn pair before and after the photo-absorption is the same. Thus, the corresponding current is isoscalar. The isovector part of the current is given by diagram c) and three analogous diagrams with photons attached at the vertices and to the other member of the pn pair. In this case photo-absorption changes the isospin state of the pn pair, generating the isovector piece of the current.

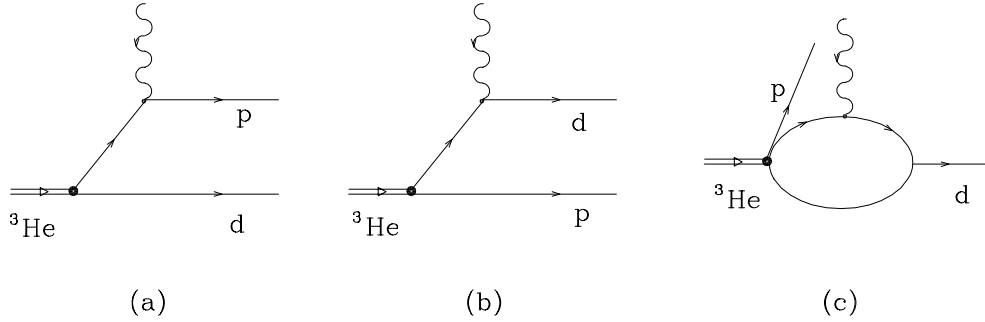


Figure 2: Leading diagrams for the ${}^3\text{He}(\vec{e}, e'd)$ process [38]: (a) proton pole, (b) deuteron pole corresponding to the quasi-deuteron model; these graphs form a part of the isoscalar current contribution; and (c) isovector current.

The ${}^3\text{He}(e, e'd)p$ channel is therefore also a source of information about the isoscalar and isovector structure of the electromagnetic current, since the contributions from individual diagrams can be suppressed or enhanced by an appropriate choice of kinematic conditions. As one-body mechanisms are strongly suppressed near the deuteron pole, the two-body piece of the current can be probed at low recoil momentum. This is in contrast to the $(e, e'p)$ channel where the two-body currents manifest themselves only at high recoil momenta which makes them difficult to investigate.

2.1 Overview of existing related measurements

In the early measurement at Bates [26], compelling evidence for the important role of the isovector current was found. In contrast to the $(e, e'p)$ channel, the isovector current introduces an interference between S and S' states in the ${}^3\text{He}(\vec{e}, e'd)$ reaction. Thus, the proposed polarized measurements of A_x and A_z in the region of $p_r = 0 - 200$ MeV/c in both parallel and perpendicular kinematics would provide much richer information on the structure of the ${}^3\text{He}$ nucleus, especially on the contribution of the S' component. Early studies of the unpolarized ${}^3\text{He}(e, e'd)$ reaction at NIKHEF and Bates [25–27] have revealed detailed information on nucleon momentum distributions, isospin structure of the currents and on final-state effects. They have also proven the need for full Faddeev calculations. Nevertheless, benefiting from the successes of these early experiments, the understanding of the three-body system could be further enhanced by spin-dependent measurements.

Using polarization degrees of freedom, the inclusive quasi-elastic ${}^3\text{He}(\vec{e}, e')$ reaction was also investigated in an effort mostly motivated by extractions of the neutron magnetic form-factor [5, 42–45]. Measurements of the induced target asymmetry A_y^0 and the asymmetry A_z were performed at NIKHEF [48, 49] in the semi-inclusive ${}^3\text{He}(\vec{e}, e'n)$ channel. This was a pilot experiment which demonstrated the feasibility of experiments with polarized ${}^3\text{He}$ internal targets, and it revealed an urgent need for strict inclusion of all rescattering effects and full Faddeev calculations.

Only one set of unpublished measurements of the exclusive ${}^3\text{He}(\vec{e}, e'd)p$ channel with a partial overlap with the proposed experiment exists from NIKHEF [50]. The statistical accuracy of these measurements was insufficient to resolve the role of the S' components at low missing momenta.

The inverse process of radiative capture $p(d, \gamma^*){}^3\text{He}$ at intermediate energies has also been studied theoretically [51–54] with direct implications for the ${}^3\text{He}(\vec{e}, e'd)$ channel. The covariant and gauge-invariant model of [52] (see also replies in [53, 54]) attempted to describe the unpolarized ${}^3\text{He}(e, e'd)$ data in parallel kinematics from NIKHEF [25] which overlaps very well with the kinematic range of the proposed measurement. The calculations revealed a rather strong sensitivity of the predictions to the ingredients of the wave-function and of the nucleon-nucleon potentials used to calculate it. The effects were more pronounced in the region of low recoil momentum, in line with the discussion on our choice of kinematics given in section 3.1.

2.2 Relation to Jefferson Lab experiments

The proposed experiment will detect deuterons ejected from a polarized ${}^3\text{He}$ target for the first time in Hall A. In this sense, it is not directly related to any of the existing or planned experiments in this Hall. However, the attempt to isolate small components of the ground-state wave-function of ${}^3\text{He}$ should prove to be beneficial to the whole ${}^3\text{He}$ -program pursued at JLab and elsewhere, in particular to experiments E-94-010, E-95-001, E-97-103, E-97-110, E-99-117, E-01-012, and E-02-013 which are presently being analyzed or yet to be performed in Hall A.

In experiments E-94-010 [18] and E-97-110 [21], the Q^2 -evolution of the spin structure function of the neutron is studied in a search for a connection between the Bjorken and Drell-Hearn-Gerasimov sum rules. In E-95-001 [19], inclusive quasi-elastic ${}^3\text{He}(\vec{e}, e')$ reaction was investigated in an effort motivated by the extraction of the neutron magnetic form-factor [5]. This can serve as a prime example of an experimental analysis that went hand-in-hand with theoretical analyses [46,47] which were in turn “gauged” by ample experimental input. Experiments E-99-117 [22] and E-97-103 [20] have also recently completed acquiring precision data on the neutron asymmetry $A_1^n(x_{\text{Bj}})$ for large x_{Bj} and on the neutron structure function $g_2^n(x, Q^2)$. The forthcoming experiment E-01-012 [23] is an extension of the $A_1^n(x_{\text{Bj}})$ measurements to the resonance region, and will establish a much better understanding of the quark-hadron duality. And experiment E-02-013 [24] plans to use polarized ${}^3\text{He}$ to measure G_n^E to high Q^2 . The expected precision of these data will need to be matched with an appropriate sophistication of the models used to extract the information on the neutron, as illustrated in figure 3.

2.3 Relation to Bates and Mainz experiments

The proposed measurement is uniquely suited to the instrumental capabilities of Hall A. The experiment can not be performed with the out-of-plane spectrometer system at MIT-

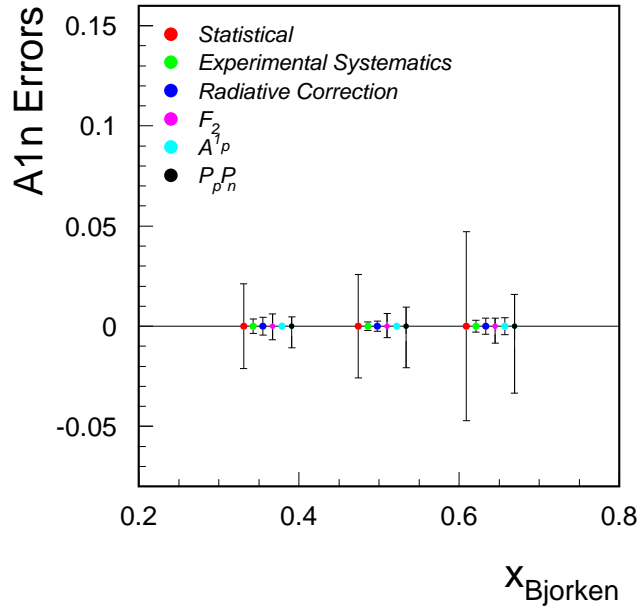


Figure 3: Shown are the errors from the recently completed E99117 A_1^n experiment [22] for different values of x_{Bjorken} . Aside from statistical error, the leading source of error is due to the uncertainty of the polarization of the proton and neutron (P_p, P_n) in polarized ^3He .

Bates since the high-density polarized ^3He target does not exist and will not be built. The BLAST detector at MIT-Bates offers the benefit of an extended acceptance which could be exploited in increasing the coverage in recoil momentum. However, the planned available luminosities at BLAST will be three orders of magnitude smaller than required here, and the figure-of-merit is small due to low beam energy. A measurement at Mainz would have similar significant disadvantages of lower beam energy, lower thickness of the polarized ^3He target, and a smaller detector acceptance.

The double-polarized ^3He electro-disintegration experiments with BLAST and at Mainz emphasize $(e, e'p)$ and $(e, e'n)$ reaction channels, mainly because their detector systems are optimized for proton and neutron detection, but not for detection of low-energy deuterons. These approaches [16,17] are largely complementary to the method of the proposed experiment. For example, while the $(e, e'p)$ channel is predicted to have sensitivity to the effects of the D-state, the $(e, e'd)$ channel is predicted to exhibit large sensitivities to effects of both S' - and D-states.

In addition, the high value of Q^2 achievable in Hall A is important in minimizing possible effects of final-state interactions, a critical issue when trying to measure small asymmetries and study small wave-function components, while keeping the Q^2 low enough that a non-relativistic treatment can be used [39].

3 Formalism of the ${}^3\text{He}(\vec{e}, e'd)p$ reaction

In the case of polarized beam and polarized target, the cross-section for the ${}^3\text{He}(\vec{e}, e'd)p$ reaction has the general form

$$\frac{d\sigma(h, \vec{S})}{d\Omega_e dE_e d\Omega_d dp_d} = \frac{d\sigma_0}{d\Omega_e dE_e d\Omega_d dp_d} \left[1 + \vec{S} \cdot \vec{A}^0 + h(A_e + \vec{S} \cdot \vec{A}) \right],$$

where σ_0 is the unpolarized cross section, \vec{S} is the spin of the target and h is the helicity of the electrons (we follow here the notation of Laget [37]). The \vec{A}^0 and A_e indicate the asymmetries induced by the polarization of only the target or only the beam, while \vec{A} is the asymmetry when both the beam and the target are polarized. The target quantization axis is chosen to be along the direction of the momentum transfer. We will focus on the asymmetry \vec{A} of which only two components $A_{x,z}$ ($\vec{S}_x \perp \vec{q}$ and $\vec{S}_z \parallel \vec{q}$) are non-zero in coplanar geometry with the spin aligned in the scattering plane,

$$A_{x,z} = \frac{[d\sigma_{++} + d\sigma_{--}] - [d\sigma_{+-} + d\sigma_{-+}]}{[d\sigma_{++} + d\sigma_{--}] + [d\sigma_{+-} + d\sigma_{-+}]} . \quad (1)$$

The (\pm, \pm) signs represent the beam helicities and the projections of the target spin along the quantization axis (x for A_x and z for A_z). Obviously, A_x and A_z have to be measured separately since they require different spin orientations. Following this four-fold spin-flip sequence, possible systematic uncertainties and contributions from \vec{A}^0 and A_e can be greatly suppressed.

3.1 Choice of kinematics

By appropriate choices of kinematic conditions, the contributions from individual diagrams in Figure 2 can be suppressed or enhanced, allowing for isoscalar/isovector parts of the currents and S' - and D -state components of the wave-function to be probed selectively.

In the quasi-elastic scattering on the proton ($e, e'p$) with an energy transfer of $\simeq -q^2/2M_p$ [30], the proton-pole diagram will dominate at low recoil momentum. It has been shown that the amplitude can be factorized exactly, and at low recoil momentum, where only the S -wave part of the vertex is retained, all information about nuclear dynamics will be canceled in the asymmetry ratio Eq. (1). In this case, the asymmetries are determined only by the electro-magnetic form-factors of the proton [37] and the reaction ${}^3\text{He}(e, e'p)d$ provides little sensitivity on the S' components, which manifest themselves only at small recoil momentum. Clearly, in the prevailing S -wave configuration, the spin direction of one proton coincides with the neutron spin orientation and, as a result, coincides with the nuclear spin. Then the proton which absorbs the virtual photon in the ${}^3\text{He}(e, e'p)d$ channel at low recoil momentum has a selected spin orientation opposite to the nuclear spin. In this case the polarized ${}^3\text{He}$ can be interpreted as a polarized proton target.

For the quasi-elastic $(e, e'd)$ reaction at an energy transfer of $\simeq -q^2/2M_d$, it is the deuteron pole which is near the “physical” region and at low recoil momentum the contributions of one-body mechanisms are strongly suppressed. Now the full amplitude defines both the isoscalar and isovector transitions. Due to their interference, no cancellation of the nuclear dynamics occurs, and the asymmetries of Eq. (1) for the ${}^3\vec{\text{He}}(\vec{e}, e'd)p$ channel will be sensitive to the S' components.

In Figures 4 and 5 the asymmetries A_x and A_z for the ${}^3\vec{\text{He}}(\vec{e}, e'd)p$ channel are plotted as functions of the recoil momentum. Figure 4 shows a full Faddeev calculation for parallel kinematics ($\vec{p}_r \parallel \vec{q}$) by the Hannover group [40]. Figure 5 shows the results of the approach by Nagorny [38] for both parallel and perpendicular kinematics ($\vec{p}_r \perp \vec{q}$). Both calculations were performed for a beam energy of 750 MeV and momentum transfer of 380 MeV/c. We show them here for comparison of sensitivities.

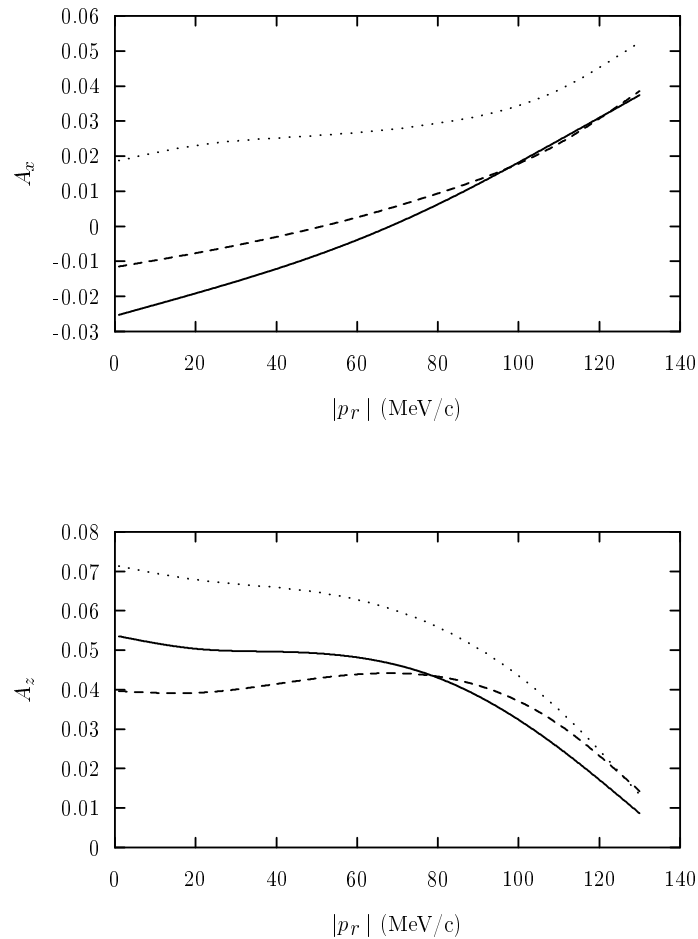


Figure 4: Full Faddeev calculation [40] of the asymmetries A_x (top) and A_z (bottom) for parallel kinematics ($\vec{p}_r \parallel \vec{q}$), for a beam energy of 750 MeV and $|\vec{q}| = 380$ MeV/c: only S state included (dotted lines), $S + S'$ states included (dashed lines), and full calculation with inclusion of $S + D + S'$ states and single Δ -isobar excitations.

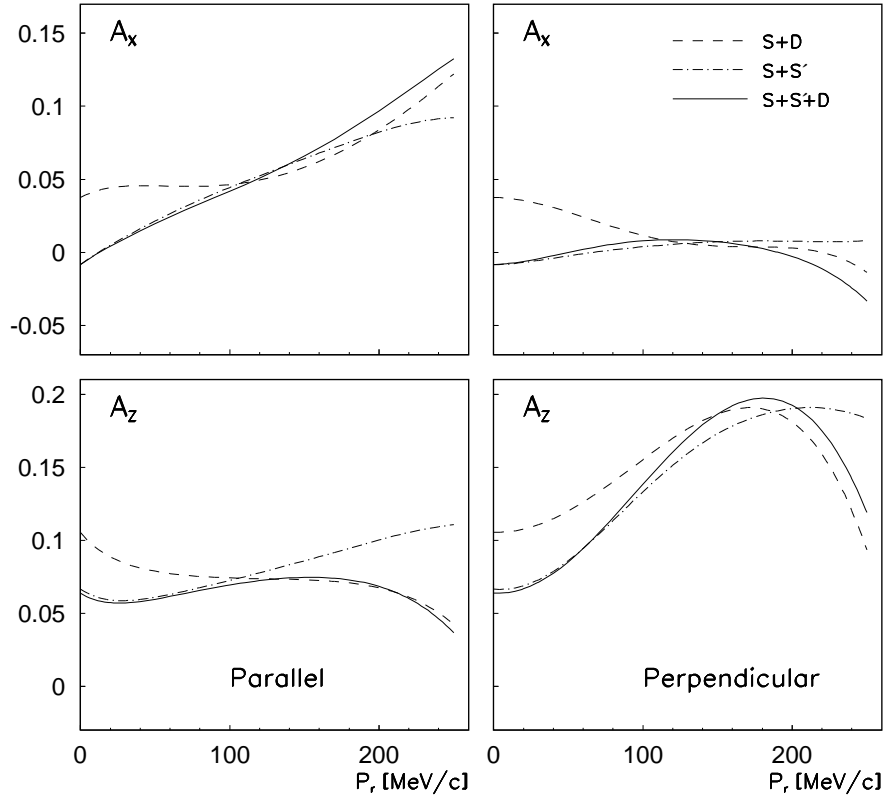


Figure 5: The asymmetries A_x and A_z for parallel ($\vec{p}_r \parallel \vec{q}$, left panel) and perpendicular ($\vec{p}_r \perp \vec{q}$, right panel) kinematics at a beam energy of 750 MeV and $|\vec{q}| = 380$ MeV/c, by Nagorny [38]: including S + D states (dashed), S + S' states (dash-dotted), and S + D + S' states (full curves).

Large effects from S' and D components arise and can easily be discerned in Figures 4 and 5 in the different regions of the recoil momentum range. There is virtually no sensitivity to either asymmetry to the S' and D components for $100 < p_r < 120$ MeV/c. This interval of recoil momenta can therefore be used to examine the effects of FSI and the isoscalar/isovector current structure of the two-body current. The calculations [38–40] make it evident that the predicted asymmetries in this interval are practically model-independent, as they are determined only by the composition of the partial waves in the momentum distribution functions which are very similar for a variety of realistic nucleon-nucleon potentials for energies up to 300 MeV/c.

Obviously, a momentum transfer of 380 MeV/c results in a low energy of knocked-out deuterons, impractical for detection from the high-density target of Hall A with relatively thick walls. We therefore opted to choose the final production kinematics with a higher $|\vec{q}|$ of about 620 MeV/c. This gives the advantage of minimizing the FSI effects compared to a lower $|\vec{q}| = 380$ MeV/c, without compromising the counting rates (or beam-time). We plan to use a beam energy of 2.4 GeV with an electron scattering angle of 15° . This results in a kinematical range with the best figure-of-merit for asymmetries and also fully exploits the kinematical coverage of the BigBite spectrometer.

Fortunately, with the beam energy of 2.4 GeV, the calculations show that the physics sensitivities remain large. Two independent full Faddeev calculations of the asymmetries A_x and A_z were performed by the Bochum group (W. Glöckle, J. Golak) [39] and by the Hannover group (P. Sauer, L. Yuan) [40]. Figures 6 and 7 show the asymmetries for the beam energy of 2.4 GeV, together with the expected uncertainties of the data. Figure 8 shows both calculations in comparison.

The role of the S' state is evident in the region of small recoil momenta, where the asymmetries are relatively flat. In the limit of $p_r = 0$, obviously the kinematics in perpendicular and parallel kinematics converge. To some extent, the asymmetries in this region are therefore neither sensitive to the magnitude of p_r nor to the kinematics. At larger recoil momenta, the importance of the D state is increasing, with asymmetries starting to change dramatically. In the Faddeev calculations of Golak [39], the effects of final-state interactions (FSI) and meson-exchange currents (MEC) are also investigated. It is apparent from Figure 7 that in general, the effects FSI and MEC are large, but the characteristic features of the asymmetries remain. Our proposed measurements will cover the entire kinematical region. The precision of the data we intend to acquire will allow us to fully test these state-of-the-art models.

We intend to acquire data on A_x and A_z with the target spin orientation in the scattering plane, in both parallel kinematics with $\vec{p}_r \parallel \vec{q}$ and perpendicular kinematics with $\vec{p}_r \perp \vec{q}$. In principle, one can also acquire data on asymmetries A_y^0 (with unpolarized beam) and A_y (with polarized beam) with the target spin oriented perpendicular to the scattering plane. However, this would require additional beam-time.

Fortunately, with the out-of-plane capability of BigBite, the asymmetry A_e (the so-called “out-of plane asymmetry” arising from the “fifth” response) can be measured simultaneously during the A_x and A_z measurements. These asymmetries (A_e , A_y^0 and A_y) are sensitive to the FSI effects and provide a means to study the spin-dependent reaction mechanism. In addition, BigBite will allow for simultaneous measurements of ${}^3\vec{\text{H}}e(\vec{e}, e'p)d$ and ${}^3\vec{\text{H}}e(\vec{e}, e'p)pn$ channels, although at the present design status of BigBite, it is not clear whether its momentum resolution will be sufficient for a clear separation of two-body and three-body breakup contributions. Possibly, the separation at low momentum transfers we require might succeed with a time-of-flight measurement (see subsection 4.4), an issue presently under investigation. A previously approved JLab experiment [35] aimed to measure proton channels, with goals that could easily be accommodated in a parasitic mode to our proposed measurements. However, we limit the scope of discussion to ${}^3\vec{\text{H}}e(\vec{e}, e'd)$ for this proposal.

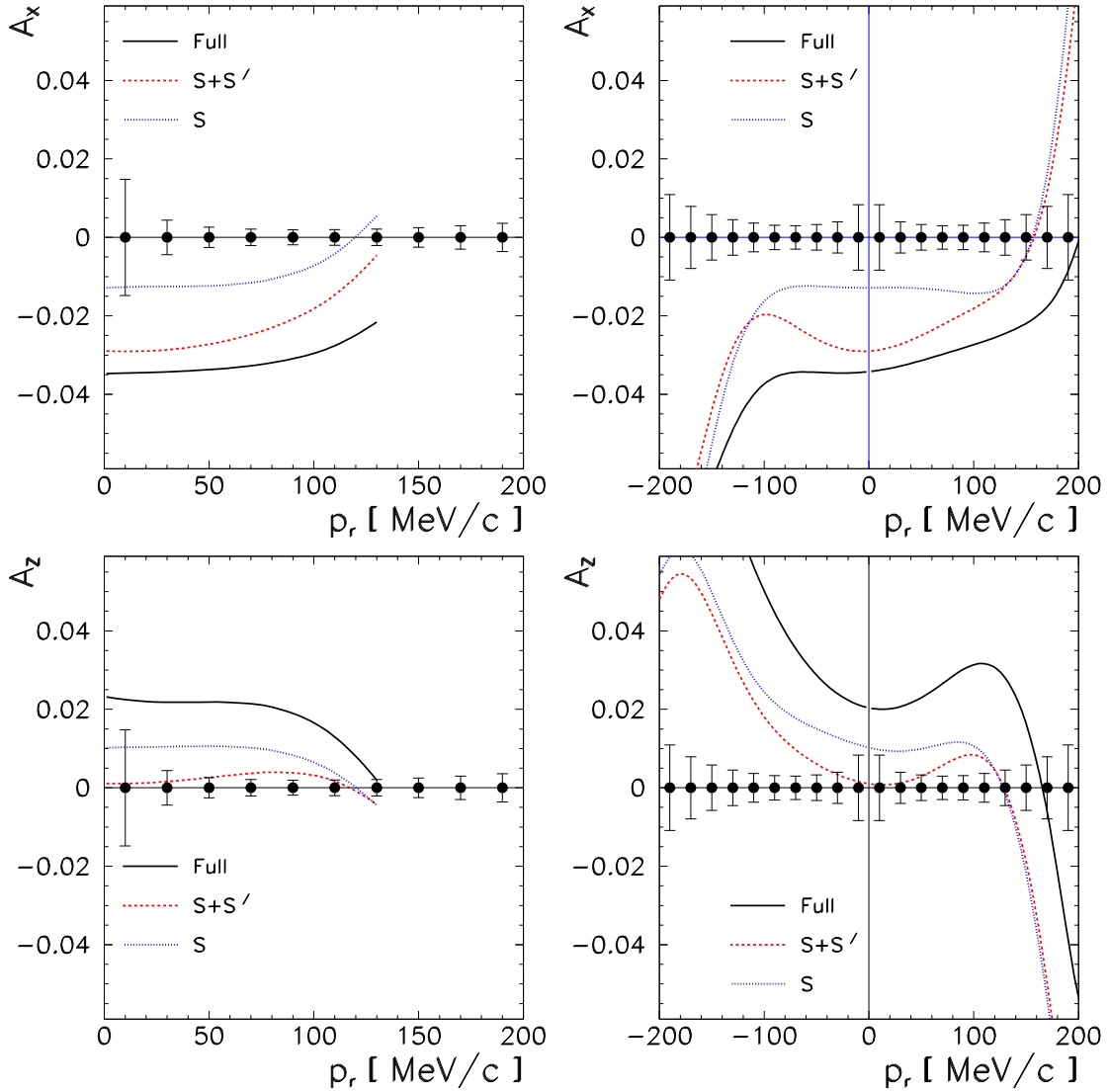


Figure 6: Asymmetries A_x and A_z for a beam energy of 2.4 GeV and $|\vec{q}| = 620$ MeV/c in parallel (left column) and perpendicular kinematics (right column) predicted by Sauer [40]: including S state (dotted curves), including S and S' states (dashed curves), and full calculation (full curves). The full calculation implies inclusion of all components (S + S' + D), as well as single Δ -isobar excitations. The expected uncertainties of the data are also shown.

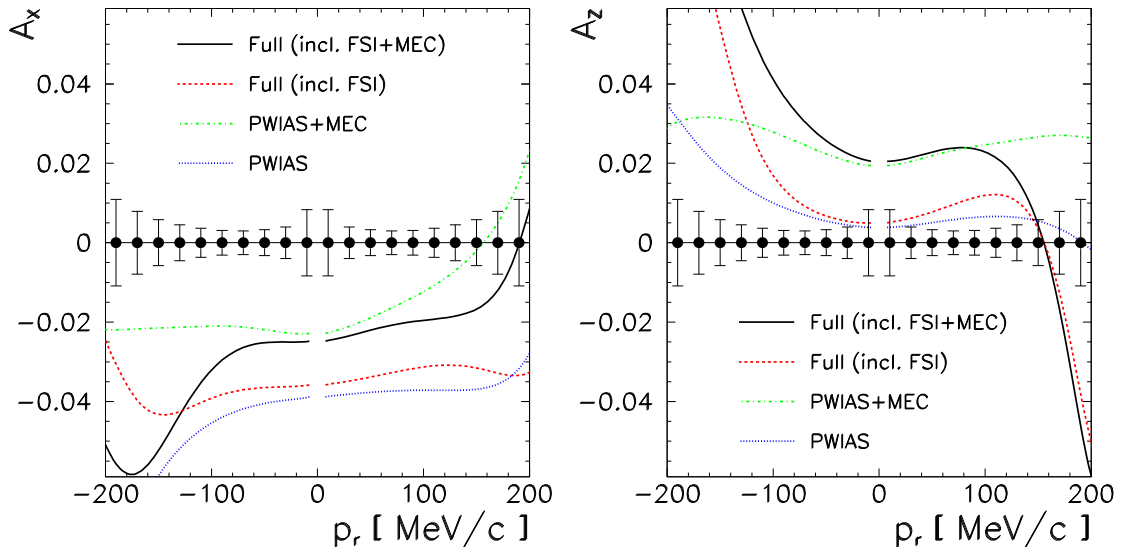


Figure 7: Asymmetries A_x and A_z for a beam energy of 2.4 GeV and $|\vec{q}| = 620$ MeV/c in perpendicular kinematics predicted by Golak [39]: PWIAS (symmetrised PWIA, dotted curves), PWIAS with inclusion of MEC (dashed-dotted curves), full calculation including FSI (dashed curves), and full calculation including FSI and MEC (full curves). The expected uncertainties of the data are also shown.

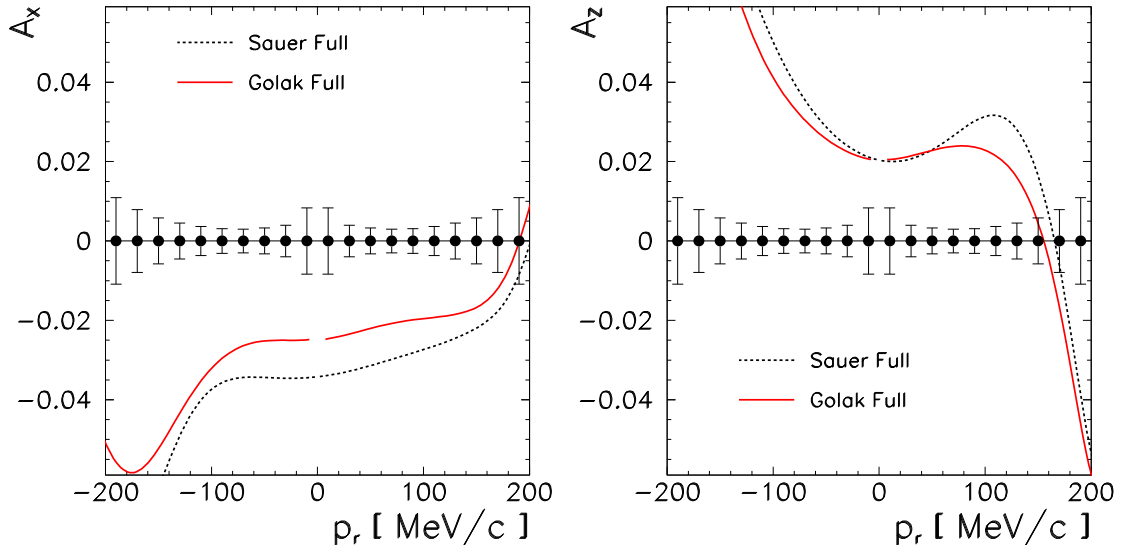


Figure 8: Comparison of full calculations by Golak [39] (full curves) and Sauer [40] (dashed curves) for a beam energy of 2.4 GeV and $|\vec{q}| = 620$ MeV/c of asymmetries A_x and A_z in perpendicular kinematics. The expected uncertainties of the data are also shown.

4 Experimental equipment and methods

We plan to use a beam energy of 2.4 GeV with an electron scattering angle of 15° , corresponding to a momentum transfer of 620 MeV/c.

We will use the standard high-pressure polarized ^3He target in Hall A and polarized beam. The scattered electrons will be detected in one of the HRS in coincidence with the knocked-out deuterons detected in the large-acceptance BigBite spectrometer. The other HRS will be used to continuously monitor the product of beam and target polarizations by detecting elastically scattered electrons at a forward angle. The layout of the detector configuration and the target spin orientations for the measurements of A_x and A_z asymmetries in the $^3\text{He}(\vec{e}, e'd)$ reaction is shown schematically in Figure 9. All directions are in the scattering (horizontal) plane. We will describe the components of experimental setup and the kinematics in detail next.

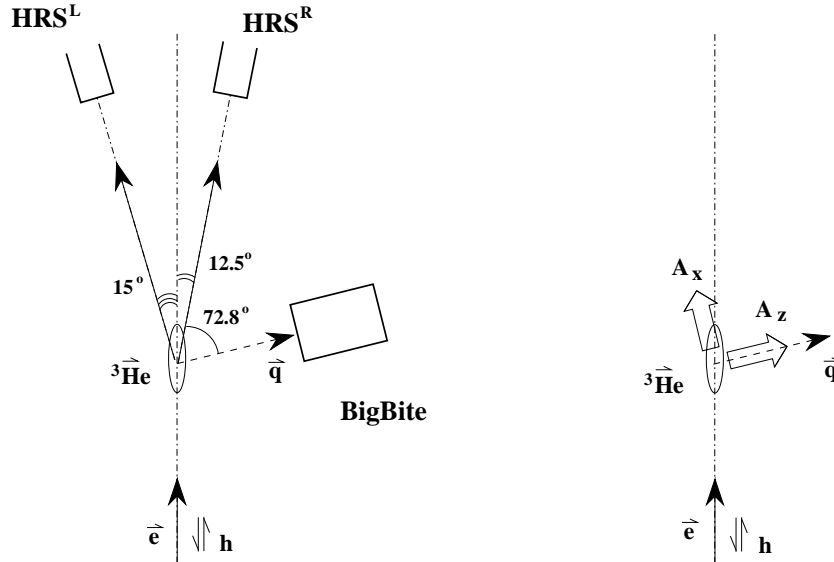


Figure 9: Schematic outline of the experimental configuration. Left: HRS^R for detecting elastically scattered electrons and HRS^L -BigBite configuration for the $^3\text{He}(\vec{e}, e'd)$ production running. Right: beam helicities and two sequential target polarization alignments for measurements of A_x and A_z .

We plan to center the BigBite spectrometer on the central momentum transfer vector as defined by the HRS spectrometer, as shown in Figure 9. This will give us a large phase-space coverage for the perpendicular kinematics with p_r up to approx. 200 MeV/c. The beam-time will be split between the target spin orientations parallel and perpendicular to the momentum transfer direction to obtain A_z and A_x . During each asymmetry measurement, the beam helicity will be fast-flipped (at 30 Hz) and the target spin will be flipped every 24 hours of data-taking to suppress possible systematic uncertainties as shown in Eq. (1).

4.1 Polarized ^3He target

We will use the high-pressure polarized ^3He target which uses optically pumped Rubidium vapor to polarize the ^3He nuclei through spin-exchange collisions [55,56]. It has been successfully used in a series of experiments in Hall A, E-94-010 [18], E-95-001 [19], and, most recently, in E-97-103 [20] and E-99-117 [22].

Optical pumping will be achieved with multiple diode lasers with a power of 30 W each, at a tunable wave-length around 795 nm. The target density will be about $2.7 \cdot 10^{20}/\text{cm}^3$ corresponding to a pressure of about 10 bar during normal operation. The target window thicknesses will be measured mechanically and optically with uncertainties better than 1.0 %, which is important for a proper understanding of radiative energy losses. The background from the nitrogen admixture will be measured by using an equivalent dummy target, and subtracted. In previous experiments, this contribution was found to be relatively small (on the order of a few percent).

The proposed experiment requires a flexible alignment of the target polarization vector parallel to (for A_z asymmetry) or perpendicular to (for A_x asymmetry) the direction of momentum transfer. Two pairs of Helmholtz coils provide the necessary quantization axis by supplying a variable static holding field of about 2 – 4 mT which can be rotated in the horizontal plane. The careful alignment of the coils assures that the polarization relaxation caused by the $\sim 1/B^2$ field inhomogeneities is minimized.

In principle, the BigBite spectrometer will introduce fringe field in the target region. Based on experience from NIKHEF and HERMES, the fringe field can be suppressed by using additional compensation magnets. Therefore, we do not think that it will represent a substantial problem for the experiment.

The target polarization P_t will be monitored with a nuclear magnetic resonance (NMR) system using the method of adiabatic fast passage (AFP). For the past experiments, the response of the NMR system for ^3He has been calibrated with the NMR measurements on water. The calibration was independently verified by measurements of the frequency shifts in the lines of electron paramagnetic resonance (EPR) spectra caused by polarized ^3He nuclei [57]. The calibration constants from these independent determinations are well known, and are consistent to within 2 %.

The expected total uncertainty from the direct polarization measurement is expected to be smaller than 4 % and will be dominated by the uncertainty in the target density. In addition to the direct measurement using NMR and EPR, P_t will also be deduced from the third independent cross-check, the measurement of elastic scattering asymmetries from ^3He discussed in more detail below. These asymmetries are sensitive to the product of the beam and target polarizations $P_e P_t$. In the recently performed experiments, all three methods were shown to give mutually consistent and reproducible results to within $(2 \pm 5)\%$.

Based on the experience of previous experiments, target polarizations of 30 – 40 % can be achieved for beam currents not exceeding 10 – 15 μA . We assume a target polarization of 35 % and a beam current of 12 μA in our rates calculations and beam-time requests.

4.2 $\vec{e}-^3\vec{\text{He}}$ elastic scattering as a polarization monitor

The product of the beam and target polarizations in the interaction region will be monitored continuously during the experiment by measuring the asymmetry in the cross-section for elastic electron- ^3He scattering. The asymmetry for scattering off a polarized ^3He target is given by [58]

$$A_{\text{elas}} = \frac{\Delta}{\Sigma} = -\frac{v'_T F_T^2 \cos \theta^* + 2v'_{TL} F_T F_L \sin \theta^* \cos \phi^*}{v_L F_L^2 + v_T F_T^2},$$

where the v and v' are kinematic factors, θ^* is the angle between the target polarization vector and \mathbf{q} , ϕ^* is the angle between the scattering plane and the spin orientation plane, and Σ and Δ are the spin-independent and spin-dependent parts of the cross section, respectively. We assume that the charge and magnetic form-factors are normalized as $F_c(Q^2 = 0) = F_m(Q^2 = 0) = 1$, so that

$$Z^2 F_c^2 = 4\pi \frac{F_L^2}{(1 + \tau)},$$

$$\mu_A^2 F_m^2 = 4\pi \frac{F_T^2}{2\tau},$$

where $\mu_A = (M_{\text{He}}/m_N)\mu(^3\text{He}) = -6.368 \text{ n.m.}$ and $\tau = Q^2/4M_{\text{He}}^2$. Since the elastic charge and magnetic form-factors of ^3He are accurately known, the measured elastic asymmetry can be used to determine the product of beam and target polarization.

With the beam energy of 2.4 GeV, electrons elastically scattered from ^3He will be detected in one of the HRS. Alternatively, since the elastically scattered electrons and the electron scattered quasi-elastically in the $^3\vec{\text{He}}(\vec{e}, e'd)p$ process have energies lying within the momentum bite of the same spectrometer, they could be detected in a single HRS.

With the 25 cm target, we anticipate a luminosity of $\approx 5.0 \cdot 10^{35}/\text{cm}^2\text{s}$ for a beam current of 12 μA , which we use henceforth. At 15° , the elastic electron- ^3He cross-section is about $6 \cdot 10^{-34} \text{ cm}^2/\text{sr}$. If the polarization measurements is done parasitically during the asymmetry measurements for the $^3\text{He}(e, e'd)p$ reaction, the elastic θ^* will be at the sub-optimal location of about 3° during the A_z measurement (with $A_{\text{elas}} = 14.74\%$), and at about 93° during the A_x measurement (with $A_{\text{elas}} = 11.94\%$) (see Figure 10). If a dedicated HRS is used to perform the polarization measurement, optimal θ^* can be adjusted when the HRS is at its minimal angle of 12.5° with the elastic cross-section of $0.03 \cdot 10^{-30} \text{ cm}^2/\text{sr}$. Assuming a beam polarization of 75%, an average target polarization of 35%, and an asymmetry of $A_{\text{elas}} = 12\%$, the product $P_e P_t$ can be measured with an accuracy of $\pm 8\%$ within one hour.

The measured elastic asymmetries will be corrected for the dilution factor which represents the fraction of scattered electrons considered to be originating from elastic collisions, compared to the total number of detected electrons. False events mostly come from the scattering of electrons off the N_2 gas in the target cell. The dilution factors found in previous experiments with polarized ^3He targets were on the order of a few percent. The beam polarization P_e will also be measured separately using Møller scattering and Compton polarimetry in the beam-line of Hall A.

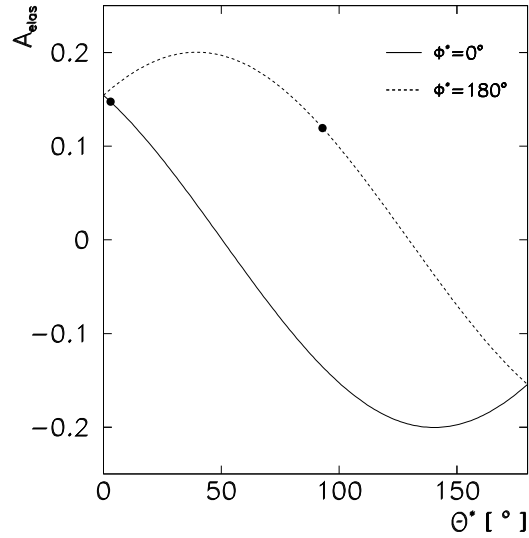


Figure 10: Asymmetries A_{elas} for elastic scattering of electrons from polarized ^3He as a function of angle θ^* between the elastic momentum transfer and the direction of target polarization. The points show the expected asymmetries if the same HRS is used for quasi-elastic and elastic scattering. If another HRS is used only for the elastic asymmetry measurement, more optimal angles can be obtained.

4.3 High-Resolution Spectrometers

The left HRS (HRS^L in Figure 9) will be used to detect the quasi-elastically scattered electrons from the $^3\text{He}(e, e'd)p$ reaction. The angular resolution is $\simeq 0.6$ mr in the non-dispersive plane and $\simeq 2.0$ mr in the dispersive plane. The momentum acceptance is $\pm 4.5\%$, and the angular acceptance is ± 60 mr in the dispersive plane and ± 22 mr in the non-dispersive plane.

The right HRS (HRS^R in Figure 9) will be used as an auxiliary spectrometer to monitor the polarization product $P_e P_t$ and luminosity throughout the experiment.

The large momentum acceptance also allows a simultaneous detection of elastically scattered electrons in HRS^L. This will give an additional elastic monitoring at a slightly different Q^2 for the polarization product $P_e P_t$.

4.4 BigBite Spectrometer

The BigBite is a non-focusing spectrometer with a large solid angle of 96 msr and a large momentum acceptance of $200 - 900$ MeV/c. It consists of a single dipole magnet followed by a detector system. In its NIKHEF version [59,60], the BigBite detector package consisted of two multi-wire drift chambers, a single scintillator layer, and a diffusely-reflecting aerogel Čerenkov detector [61]. For its much broader application as the third arm of the spectrometer setup in Hall A, BigBite will be upgraded in order to be capable of

handling larger single rates. The simulations of the expected detector performance have shown that the scintillator system of BigBite will allow for excellent discrimination between deuterons, protons, and unresolved kaons and pions on the basis of time-of-flight measurement alone (see Figure 12) especially for deuteron momenta of 300 – 900 MeV/c optimal for our proposal.

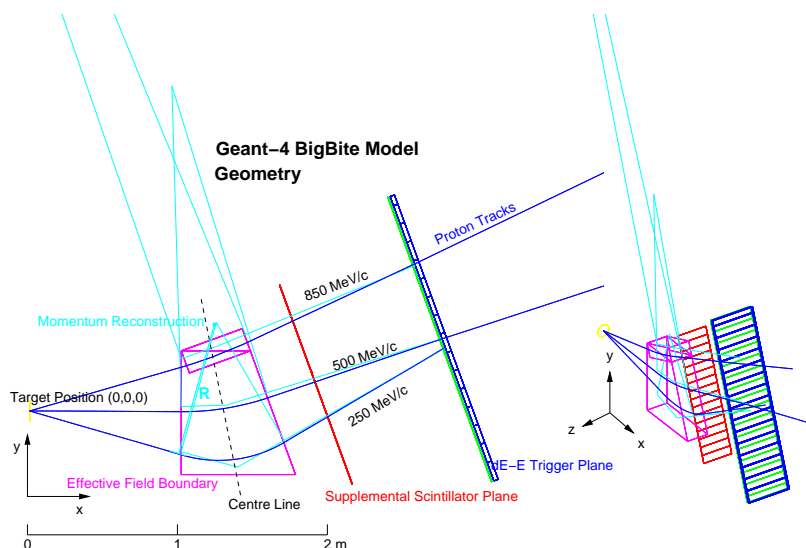


Figure 11: Schematic view of BigBite including the first stage of the planned upgrade with installation of segmented time-of-flight detectors.

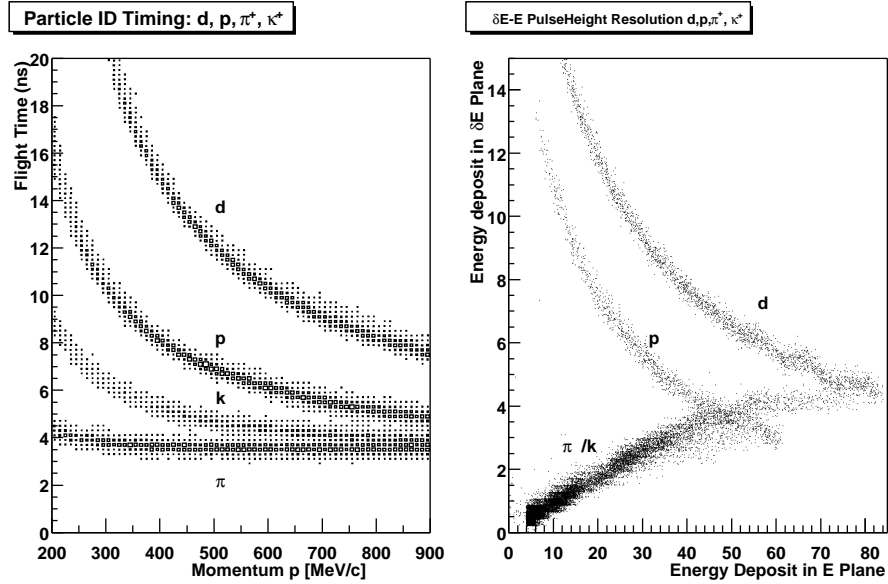


Figure 12: Simulated particle identification performance of BigBite using only the time-of-flight measurement. In the left panel, the four bands from bottom to top correspond to unseparated electrons and pions, kaons, protons, and deuterons, respectively. On the right, the $\delta E - E$ pulse-height resolution is shown for the same particle types with the deuteron band well separated.

5 Count rates and beam time request

The proposed kinematics, the estimated count rates and the beam-time allocation are shown in Tables 1, 2, and 3. The counting rates and statistical uncertainties were calculated using the Hall A Monte Carlo code MCEEP [63]. For single rates in the HRS, we assume a luminosity of $\approx 5.0 \cdot 10^{35}/\text{cm}^2\text{s}$ for a beam current of $12 \mu\text{A}$. However, the limited extended-target acceptance of BigBite (about ± 10 cm at 90° and 1 m drift distance) reduces the useful luminosity for BigBite to $\approx 4.0 \cdot 10^{35}/\text{cm}^2\text{s}$. The measured ${}^3\text{He}(e, e'd)p$ cross-sections from NIKHEF at low Q^2 and the calculated cross-sections at high Q^2 , and the off-shell $e - d$ cross-section [64] were used in the MCEEP simulation. In the simulation, we also accounted for the HRS and BigBite inefficiency in y_{tg} . Thus the rates as well as the beam-time estimates are considered to be very realistic. The estimated single count rates and accidental coincidence rates are also shown in Table 2. In order to accommodate radiation losses, we request additional 20 % beam-time, as shown in Table 3.

We intend to use the BigBite spectrometer at the standard drift distance of 1 m and emphasize measurements in both parallel and perpendicular kinematics. The BigBite's momentum acceptance of 250 – 900 MeV/c will cover the complete range of recoil momenta 0 – 200 MeV/c for the parallel kinematics. The angular acceptance is shown in Figure 13. This will give data for perpendicular kinematics simultaneously without additional beam-time request.

The simulated distributions of events in recoil momentum for parallel and perpendicu-

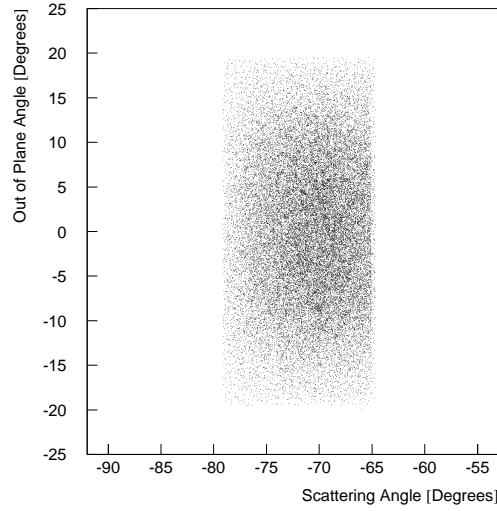


Figure 13: Simulated event angular distribution.

lar kinematics are shown in Figure 14. To select parallel kinematics in the Monte Carlo simulation, the relative angle $\theta_{p_r, \vec{q}}$ between the recoil momentum and \vec{q} was constrained to $\theta_{p_r, \vec{q}} < 30^\circ$. For perpendicular kinematics, we used $|\theta_{p_r, \vec{q}} - 90^\circ| < 30^\circ$. In the limit of $p_r = 0$, the kinematics converge, so the cuts do not influence the physics sensitivity. As shown in Figure 14, due to large momentum acceptance of BigBite, the p_r -coverage extends beyond 200 MeV/c in parallel kinematics. For perpendicular kinematics, which will be measured simultaneously, the coverage is shown in Figure 14.

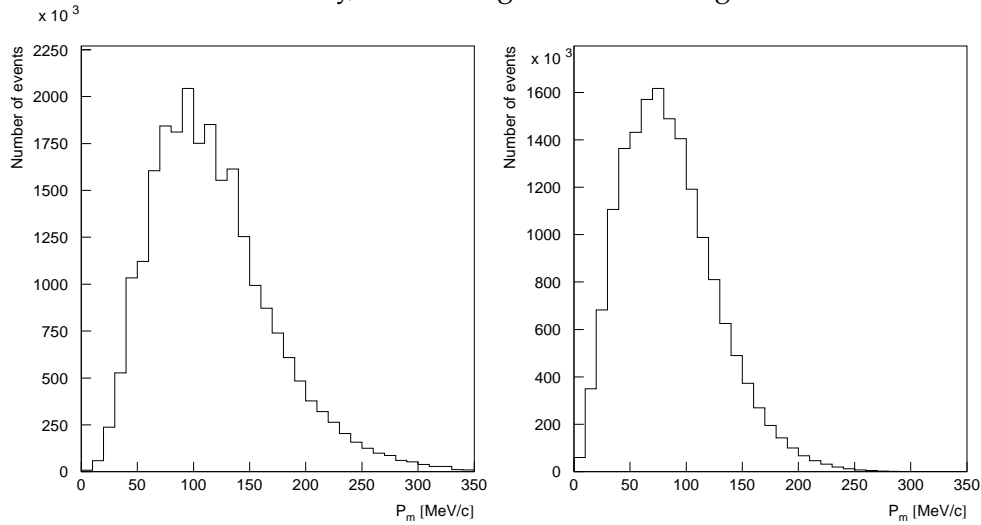


Figure 14: Simulated distribution of events in recoil momentum. Left: parallel kinematics. Right: perpendicular kinematics.

The measured asymmetries A_x^{exp} and A_z^{exp} will be given by

$$A_{x,z}^{\text{exp}} = P_e P_t A_{x,z}.$$

Thus, the statistical errors will be amplified by a factor of $1/(P_e P_t)^2$ which is approximately 15 with a 75 %-polarized beam and a 35 %-polarized target. The final statistical errors on the physical asymmetries are shown in Table 1. Note that possible measurements in perpendicular kinematics and/or utilizing the out-of-plane coverage of BigBite to access A_e , A_{LT} and A_{TT} , as well as to perform simultaneous measurements of other reaction channels can be considered, as it has been discussed above.

The amount of beam time required is driven by the counting rate in two regions of recoil momenta. At large p_r , the cross-section decreases rapidly. At small p_r , the phase-space is reduced due to the p_r^2 factor.

The statistical uncertainties of our proposed data are plotted in Figures 6, 7, and 8 in comparison to calculations. The statistical errors dominate in this experiment. The systematic errors are mainly caused by the uncertainties in the polarization of the beam ($\lesssim 2\%$) and target ($\lesssim 4\%$). Since the absolute values of the asymmetries are mostly smaller than 0.06, these uncertainties contribute only insignificantly (on the order of 0.0003) to the absolute uncertainties on the asymmetries (see Table 1).

Table 1: Estimates of event count rates and statistical errors on the asymmetries for the total requested beam time.

p_r [MeV/c]	Counts/hour in \parallel	Counts/hour in \perp	$\delta A_{x,z}^{\parallel}$	$\delta A_{x,z}^{\perp}$
10	0.29 k	1.78 k	0.0148	0.0059
30	3.33 k	7.77 k	0.0044	0.0028
50	9.37 k	12.15 k	0.0026	0.0023
70	14.99 k	13.86 k	0.0019	0.0021
90	16.76 k	12.58 k	0.0020	0.0022
110	15.67 k	9.48 k	0.0021	0.0032
130	13.78 k	6.24 k	0.0025	0.0041
150	9.77 k	3.75 k	0.0030	0.0056
170	7.01 k	2.02 k	0.0036	0.0077
190	4.75 k	1.06 k	0.0046	0.0113
Systematical	uncertainty		< 0.0003	< 0.0003

The single count rates were estimated with the computer codes QFS and EPC of Lightbody and O'Connell [65]². The single count rates in the HRS originating from the (e, d) reaction were estimated by using the Monte Carlo method simulation of ${}^3\text{He}(e, e'd)p$ and integrating the rates over the acceptance for scattered electrons. Accidental coincidence rates were calculated assuming a coincidence timing width of 2 ns and a duty factor of 100 %. The accidental rate given in the table is averaged over the whole range of missing

²The proton singles rates peak at lowest momenta. The breakdown is roughly 20.0 kHz at $p = 400$ MeV/c, 12.5 kHz ($p = 500$ MeV/c), 5.0 kHz ($p = 600$ MeV/c), 1.2 kHz ($p = 700$ MeV/c), and 0.5 kHz ($p = 800$ MeV/c).

Table 2: Proposed kinematics with a beam energy of 2400 MeV and estimates of singles and accidental rates. The Left HRS is used for production running, the Right HRS is used for monitoring of the luminosity and the product of beam and target polarizations.

		Singles				Accidentals
		(e, e')	(e, d)	(e, p)	(e, π^+)	(e, e'd)
	central kinematics	[Hz]	[Hz]	[kHz]	[kHz]	[1/hr]
HRS L	$\theta_e = 15.0^\circ$ $E' = 2294 \text{ MeV}/c$	300				
HRS R	$\theta_e = 12.5^\circ$ $E' = 2332 \text{ MeV}/c$	1300				
BigBite	$\theta_d = 72.8^\circ$ $p_d = 300 - 900 \text{ MeV}/c$ $p_r = 0 - 200 \text{ MeV}/c$		280	40	12	< 10

energies covered by the momentum acceptances of the spectrometers. Since the deuterons detected in BigBite can be clearly identified, the accidental coincidence rates from (e, p) and (e, π^+) processes are not included. When the reaction ${}^3\text{He}(e, e'd)p$ is selected, a cut on the two-body breakup peak is applied. The accidentals within the cut will be about a factor of 20 less abundant than the ones given in the table. As shown in Table 2, the accidental coincidence rate is insignificant compared to the true coincident rates. Table 3 summarizes our beam-time request.

Table 3: Beam-time allocation.

	Beam-time [days]	Radiative loss [days]	Total beam-time [days]
A_x	5.5	1.5	7.0
A_z	5.5	1.5	7.0
Calibrations	1.0	N/A	1.0
			15.0

6 Summary

We intend to obtain precision data on asymmetries A_x and A_z in the range of p_r from 0 to about 200 MeV/c in both parallel and perpendicular kinematics. We believe that the S' and D components of the ground-state wave-function of ${}^3\text{He}$ can be optimally accessed in the ${}^3\text{He}(\vec{e}, e'd)p$ reaction in quasi-elastic kinematics. This set of data will provide detailed knowledge of the ground-state spin structure of ${}^3\text{He}$, especially the S' state in the region of low recoil momentum. Our data will constitute a stringent test of the state-of-the-art Faddeev calculations which require an exact understanding of the D and S' states in ${}^3\text{He}$, which is one of the key nuclei of the “standard model” of few-body theory.

A beam energy of 2.4 GeV and the polarized ${}^3\text{He}$ target of Hall A will be used, in conjunction with the two standard HRS of Hall A and the new BigBite spectrometer. We request 15 days of beam-time.

This proposal is based on the favorable deferral of PAC 21 (see appendix A) and the Letter of Intent Review by PAC 20 (see appendix B). It has been endorsed by the entire Hall A Collaboration, especially the BigBite Collaboration and the Polarized ${}^3\text{He}$ Collaboration and has theory support from the Bochum and Hannover groups.

A PAC 21 proposal report

Motivation: The proposal aims at testing modern Faddeev calculations with emphasis on the S' and D states of the ${}^3\text{He}$. Such calculations are needed for the interpretation of experiments such of Deep-Inelastic Scattering and neutron form-factor measurements that use polarized ${}^3\text{He}$ as a polarized neutron target.

Measurement and Feasibility: The double-polarization asymmetries A_x and A_z in the ${}^3\text{He}(\vec{e}, e'd)$ reaction would be determined in both parallel and perpendicular kinematics for a range of recoil momentum. A value of 620 MeV/c is chosen for the three-momentum transfer, large enough that the produced deuterons suffer small energy loss in the target, and still within the range where relativistic effects in the Faddeev calculations are not too large. The experiment would use the hall A polarized target, one of the HRS spectrometers for the detection of the scattered electron, the other one monitoring the product of target and beam polarization, and the Bigbite spectrometer for the detection of the deuteron. Due to the relatively high luminosity of this set-up in combination with a large virtual photon flux, the count rates would be large enough to determine the small asymmetries with good accuracy. The A_x and A_z in the two kinematics show a different sensitivity to ingredients of the calculations such as the S' and D states, meson-exchange currents, and Delta-isobar currents.

Issues: It was noted that no time was asked for tests and calibrations, e.g., of the absolute angle of BigBite. By also using the data with the angle between the momentum transfer and the recoil momentum between 30 and 60 degrees, the PAC thinks that the goals of the proposals could be reached with less beam time.

The PAC would like to see this experiment performed, but due to limitations in the available beam time the proposal cannot be accepted at this time.

Recommendation: Defer

B PAC 20 letter of intent report

The motivation of the experiment is two-fold: (1) a determination of the effect of the S' component of the ${}^3\text{He}$ wave function, and (2) the isolation of the isovector interaction current contributions. The measurements would utilize a longitudinally polarized electron beam and a ${}^3\text{He}$ target polarized either longitudinally (z) or sideways (x) relative to the q axis. The scattered electron is detected in an HRS and the ejected deuteron is detected in the BigBite spectrometer. The claim is that for recoil momenta less than 50 MeV/c, the D-state will be highly suppressed so that the asymmetries will be sensitive to the interference between S and S' states. Also, the isovector component of the interaction current will be disentangled in measurements at a recoil momentum of 100 MeV/c, where the asymmetries are expected to be independent of the wave function.

The PAC endorses the first motivation, since knowledge of the effect of small components of the ${}^3\text{He}$ wave function is essential in making the transition from a polarized ${}^3\text{He}$ target to a polarized neutron. We encourage the proponents to develop a full proposal and to enlist the support of few-body theory groups (such as the Bochum group) to obtain full Faddeev calculations of the reaction as a guide in selecting the kinematics and interpreting the results. We call to their attention the report of PAC 18 on PR-00-106, which had similar goals and which was deferred due to lack of theoretical guidance. The PAC is less interested in the second motivation, since it believes that the isovector part of the interaction current has already been well studied in experiments at NIKHEF and Bates.

References

- [1] J. Carlson, R. Schiavilla, *Rev. Mod. Phys.* **70** (1998) 743.
- [2] H. Gao, *Nucl. Phys. A* **631** (1998) 170c.
- [3] J. L. Friar et al., *Phys. Rev. C* **42** (1990) 2310.
- [4] R. G. Milner, in *Proceedings of the Workshop on Polarized ^3He Beams and Targets*, R. W. Dunford, F. P. Calaprice (eds.), AIP 131, New York, 1984, p. 186.
- [5] W. Xu et al., *Phys. Rev. Lett.* **85** (2000) 2900.
- [6] M. Meyerhoff et al., *Phys. Lett. B* **327** (1994) 201.
- [7] J. Becker et al., *Eur. Phys. J. A* **6** (1999) 329.
- [8] D. Rohe et al., *Phys. Rev. Lett.* **83** (1999) 4257.
- [9] P. L. Anthony et al., *Phys. Rev. Lett.* **71** (1993) 959.
- [10] K. Abe et al., *Phys. Rev. Lett.* **79** (1997) 26, and references therein.
- [11] K. Ackerstaff, *Phys. Lett. B* **404** (1997) 383.
- [12] B. Blankleider and R. M. Woloshyn, *Phys. Rev. C* **29** (1984) 539.
- [13] R. W. Schulze and P. U. Sauer, *Phys. Rev. C* **48** (1993) 38.
- [14] J. Friar, in *Electronuclear Physics with Internal Targets and the BLAST Detector*, R. Alarcon and M. Butler (eds.), World Scientific, Singapore, 1993, p. 210.
- [15] J. L. Friar, B. F. Gibson, C. R. Chen, and G. L. Payne, *Phys. Lett. B* **161** (1985) 241.
- [16] K. McIlahny, R. Milner (spokespersons), Update to the Bates Proposal 89–12, “*Measurement of spin-dependent quasi-elastic electron scattering from polarized ^3He* ”, 2000 [approved, not yet scheduled].
- [17] R. Neuhausen (spokesperson), MAMI Proposal A1/2–00, “*The structure of ^3He* ”, 2000 [approved, not yet scheduled].
- [18] Z. E. Meziani, G. Cates, J.-P. Chen (spokespersons), JLab Experiment E–94–010, “*Measurement of the neutron (^3He) spin structure function at low Q^2 ; a connection between the Bjorken and Drell-Hearn-Gerasimov sum rules*”, 1994 [completed].
- [19] H. Gao, J. O. Hansen (spokespersons), JLab Experiment E–95–001, “*Precise measurements of the inclusive spin-dependent quasi-elastic transverse asymmetry A_T^1 from $^3\text{He}(e, e')$ at low Q^2* ”, 1995 [completed].
- [20] T. Averett, W. Korsch (spokespersons), JLab Experiment E–97–103, “*Search for higher-twist effects in the neutron spin structure function $g_2^n(x, Q^2)$* ”, 1997 [analysis underway].

- [21] J.-P. Chen, A. Deur, F. Garibaldi (spokespersons), JLab Experiment E-97-110, "The GDH rule and the spin structure of ^3He and the neutron using nearly real photons, 1997 [approved, scheduled].
- [22] Z. E. Meziani, J.-P. Chen, P. Souder, JLab Experiment E-99-117, "Precision measurement of the neutron asymmetry A_1^n at large x using CEBAF at 6 GeV", 1999 [analysis underway].
- [23] N. Liyanage, J.-P. Chen, S. Choi (spokespersons), JLab Experiment E-01-012, "Measurement of neutron (^3He) spin structure functions in the resonance region", 2001 [approved, not yet scheduled].
- [24] G. Cates, K. McCormick, B. Reitz, B. Wojtsekhowski (spokespersons), JLab Experiment E-02-013, "Measurement of the Neutron electric form Factor G_{En} at High Q^2 ", 2002 [approved, not yet scheduled].
- [25] P. H. M. Keizer et al., Phys. Lett. B **157** (1985) 255.
- [26] C. Tripp et al., Phys. Rev. Lett. **76** (1996) 885.
- [27] C. M. Spaltro et al., Phys. Rev. Lett. **81** (1998) 2870.
- [28] E. van Meijgaard, J. A. Tjon, Phys. Rev. C **42** (1990) 74.
- [29] E. van Meijgaard, J. A. Tjon, Phys. Rev. C **42** (1990) 96.
- [30] S. I. Nagornyi, Yu. A. Kasatkin, V. A. Zolenko, Phys. At. Nucl. **57** (1994) 940.
- [31] J. Golak et al., Phys. Rev. C **51** (1995) 1638.
- [32] R. G. Milner et al., Phys. Lett. B **379** (1996) 67.
- [33] C. Bloch et al., Nucl. Instr. Meth. A **354** (1995) 437.
- [34] J. F. J. van den Brand, C. W. de Jager (spokespersons), NIKHEF experiment 94-05, "Measurement of quasi-elastic spin-dependent electron scattering from a polarized ^3He internal target", 1994 [completed].
- [35] F. W. Hersman (spokesperson), JLab Proposal PR-94-023, "Measurement of small components of the ^3He wave-function using $^3\vec{\text{He}}(\vec{e}, e'p)$ in Hall A", 1994 [approved, but dropped due to jeopardy].
- [36] W. Korsch, R. McKeown, Z.-E. Meziani (spokespersons), JLab proposal PR-94-020, "Investigation of the ^3He wave-function using the $^3\vec{\text{He}}(\vec{e}, e'p)d$ and $^3\vec{\text{He}}(\vec{e}, e'p)pn$ reactions", 1994 [rejected].
- [37] J.-M. Laget, Phys. Lett. B **276** (1992) 398.
- [38] S. Nagorny, W. Turchinets, Phys. Lett. B **389** (1996) 429.
- [39] W. Glöckle, J. Golak, private communication.

- [40] L. Yuan, P. Sauer, private communication.
- [41] S. Nagorny, W. Turchinets, *Phys. Lett. B* **429** (1998) 222.
- [42] C. E. Woodward et al., *Phys. Rev. Lett.* **65** (1990) 698.
- [43] C. E. Jones et al., *Phys. Rev. C* **47** (1993) 110.
- [44] J.-O. Hansen et al., *Phys. Rev. Lett.* **74** (1995) 654.
- [45] F. Xiong et al., *Phys. Rev. Lett.* **87** (2001) 242501.
- [46] S. Ishikawa et al., *Phys. Rev. C* **57** (1998) 39.
- [47] J. Golak et al., *Phys. Rev. C* **63** (2001) 034006.
- [48] H. R. Poolman, Doctoral Dissertation, Vrije Universiteit te Amsterdam, 1999.
- [49] H. R. Poolman et al., *Phys. Rev. Lett.* **84** (2000) 3855.
- [50] E. Six, Doctoral Dissertation, Arizona State University, 1999.
- [51] J. Golak et al., *Phys. Rev. Lett.* **62** (2000) 054005.
- [52] A. Yu. Korchin, D. Van Neck, O. Scholten, W. Waroquier, *Phys. Rev. C* **59** (1999) 1890.
- [53] S. Nagorny, *Phys. Rev. C* **63** (2000) 019801.
- [54] A. Yu. Korchin, D. Van Neck, O. Scholten, W. Waroquier, *Phys. Rev. C* **63** (2000) 019802.
- [55] T. G. Walker, W. Happer, *Rev. Mod. Phys.* **69** (1997) 629.
- [56] S. Appelt et al., *Phys. Rev. A* **58** (1998) 1412.
- [57] M. V. Romalis, G. D. Cates, *Phys. Rev. A* **58** (1998) 3004.
- [58] T. W. Donnelly, A. S. Raskin, *Ann. Phys.* **169** (1986) 247.
- [59] D. J. J. de Lange et al., *Nucl. Instr. Meth. A* **406** (1998) 182.
- [60] D. J. J. de Lange et al., *Nucl. Instr. Meth. A* **412** (1998) 254.
- [61] D. W. Higinbotham, *Nucl. Instr. Meth. A* **414** (1998) 332.
- [62] J. R. M. Annand, D. Hamilton, "*Geant4/C++ Monte Carlo studies of the Big-Bite focal-plane detector systems*", preliminary report, web-version available at <http://hallaweb.jlab.org/equipment/BigBite/index.html>, 2001.
- [63] P. E. Ulmer, *MCEEP: Monte Carlo for electro-nuclear coincidence experiments*, version 3.5 (2001).
- [64] R. Ent, Doctoral Dissertation, Vrije Universiteit te Amsterdam, 1989, and private communication.
- [65] J. Lightbody and J. S. O'Connell, *Computers in Physics* **2** (1988) 57.